



universität
wien

DIPLOMARBEIT

Titel der Diplomarbeit

Characterization of RNase J in
Sulfolobus acidocaldarius

Verfasser

Lukas ZEICHEN

angestrebter akademischer Grad

Magister Naturwissenschaften (Mag.rer.nat.)

Wien, 2012, 27.Februar.

Studienkennzahl lt. Studienblatt:

A 490

Studienrichtung lt. Studienblatt:

Diplomstudium Molekulare Biologie

Betreuerin / Betreuer:

Prof. Dr. Udo Bläsi

It's not that I'm so smart, it's just that I stay with problems longer.

-Albert Einstein (1879-1955)

Index of Contents

1. Abstract	5
2. Zusammenfassung	6
3. Introduction.....	7
3.1. RNA degradation.....	7
3.1.1. <i>RNA degradation in Bacteria</i>	7
3.1.1.1. <i>RNA degradation in Gram-negative Bacteria</i>	8
3.1.1.2. <i>RNA degradation in Gram-positive Bacteria</i>	8
3.1.2. <i>RNA degradation in Eukaryotes</i>	9
3.1.3. <i>RNA degradation in Archaea</i>	10
3.2. <i>Structure of the RNase J orthologue in Sso</i>	12
3.2.1. <i>Enzymatic properties of Sso-RNase J</i>	15
3.3. <i>a/eIF2 (γ) counteracts 5' to 3' mRNA decay</i>	16
4. Aims of the study	19
5. Materials and Methods	20
5.1. Bacterial strains and plasmids.....	20
5.2. Construction of plasmids	23
5.2.1. <i>pET-28b</i>	23
5.3. Purification of SacI-RNase J and a/eIF2 (γ)	23
5.4. Preparation of RNA substrates.....	24
5.5. Labelling of DNA oligonucleotides.....	25
5.6. Enzyme assays with SacI-RNase J.....	26
5.7. Test for RNase activity in SacI extracts.....	26
5.9. Construction of the <i>S. acidocaldarius</i> Δ 2362 deletion mutant	27
5.9.1. Construction of the <i>Saci_2362</i> deletion plasmid	27
5.9.2. Construction of the <i>S.acidocaldarius</i> MW001 Δ 2362 mutant	28
5.10. High-throughput-sequencing	28

6. Results	30
6.1. SacI-RNase J	30
6.1.1. Purification of SacI-RNase J	30
6.1.2. Enzymatic properties of SacI-RNase J.....	31
6.1.3. SacI-RNase J displays 5'-to 3' exonuclease activity.....	32
6.2. Protection of the RNA 5'-terminus by α /eIF2 (γ)	33
6.4. Characterization of the <i>S. acidocaldarius</i> Δ 2362 (RNase J deletion) strain	34
6.4. 1 Differentially expressed genes in <i>S. acidocaldarius</i> MW001 and MW001 Δ 2362.....	36
7. Discussion	42
8. Appendix	49
8.1. Buffers and solutions.....	49
8.2. General protocols.....	52
9. References	54
Appendix II.....	60
Curriculum Vitae	75

1. Abstract

In Archaea the exosome is a 3'-to- 5' RNA processing and degradation machinery. However, recent studies identified a 5'-to- 3' exoribonuclease termed Sso-RNase J in the crenarchaeum *Sulfolobus solfataricus* (Sso). Here, we characterized a Sso-RNase J orthologue in *Sulfolobus acidocaldarius* (Sacl-RNase J), which comprises typical signature motifs of the β -CASP family of metallo- β -lactamases. Our studies revealed the similarities between Sso-RNase J and Sacl-RNase J and suggest a conserved 5'-to- 3' degradation process in the crenarchaeal clade of Archaea. In addition, we showed that binding of translation initiation factor α /eIF2 (γ) to the 5'-end of RNA counteracts the 5'-to- 3' exoribonucleolytic activity of Sacl-RNase J *in vitro*.

To address the biological significance of the RNase J orthologue in *S. acidocaldarius*, a deletion mutant strain was constructed and the effect of Sacl-RNase J on the transcriptome was studied by high throughput RNA sequencing. The absence of Sacl-RNases J revealed 667 genes whose transcript abundance was either increased or decreased, suggesting a complex role of this ribonuclease in both degradative and regulatory processing events.

2. Zusammenfassung

Das Exosome ist die wichtigste 3'-zu-5' RNA Prozessierungs- und Degradierungsmaschinerie in Archaea. Zusätzlich wurde kürzlich eine Exoribonuclease in *Sulfolobus solfataricus* (Sso-RNase J) identifiziert. In dieser Arbeit charakterisierten wir ein Sso-RNase J ortholog in *Sulfolobus acidocaldarius* (Sacl-RNase J), die eine 5' → 3' Exonucleaseaktivität aufwies. Diese Arbeiten zeigten, dass beide Enzyme gleiche Eigenschaften aufweisen und somit ist anzunehmen, dass ein RNA Abauprozess mit 5' → 3' Direktionalität in Crenarcheoten vorhanden ist. Zusätzlich wurde gezeigt, dass die Bindung des Translationalen Initiations Faktors αeIF2 (γ) an das 5'-Ende der RNA einen 5 → 3' Abbau durch Sacl-Rnase J inhibiert.

Um die biologische Relevanz von RNase J in Crenarcheoten näher zu beleuchten, wurde eine Sacl-RNase J Deletationsmutante konstruiert und das Transkriptom mittels „high throughput RNA sequencing“ analysiert. In Abwesenheit von Sacl-RNases J wurden 667 Gene detektiert, deren Transkripte häufiger bzw. weniger häufig vorkamen. Dies deutet auf eine komplexe Rolle der Rnase J im RNA Metabolismus von Crenarcheoten hin.

3. Introduction

There are three domains of life: Eukaryotes, Bacteria and Archaea. Archaea are notable for the extreme ecological niches, which they are able to occupy. We have chosen *Sulfolobus acidocaldarius* and *Sulfolobus solfataricus*, respectively, as model organisms for investigating mechanisms of RNA degradation. These thermophilic *Archaea* grow optimally at 75°C and at a pH of 2-3. These organisms, growing under extreme conditions are an interesting source for stable enzymes, and as a consequence a relevant tool for biotechnology [1].

These studies are focusing on mRNA degradation, i.e. on enzymes involved in decay as well as proteins stabilizing mRNA. The maturation and degradation of mRNA is a highly regulated process in all three kingdoms of life. By regulating mRNA decay, cells control gene expression, react rapidly to changing environmental conditions and can respond to stresses. Therefore the pathways leading to RNA decay have been intensively studied in Bacteria and Eukaryotes, whereas the mechanism of mRNA turnover in Archaea is poorly understood. The stability of RNA transcripts is mostly controlled by a combination of endo- and exonucleolytic activity as well as by RNA binding proteins, which can exert a protective function.

3.1. RNA degradation

Several studies have identified a number of parallels between the mRNA decay mechanisms in eukaryotic and bacterial mRNA degradation. Nevertheless, some key distinctions remain, as the structure and organization of bacterial and eukaryotic mRNAs differ in a number of significant ways. In those two kingdoms of life the stability of mRNA is highly dependent on the 5'-end. In both, degradation is known to start at the 5'- as well as at the 3'-ends of RNA [2].

3.1.1. RNA degradation in Bacteria

In Bacteria a tri-phosphorylated 5'-end and/or a 5'-terminal stem-loop structure on mRNAs can counteract the activities of RNases. The canonical model for mRNA degradation in bacterial cells was deduced from studies in *E. coli*. and it

has become apparent, that these processes differ in Gram-positive bacteria [2, 3].

3.1.1.1. RNA degradation in Gram-negative Bacteria

As *Escherichia coli* appears to lack a 5'-exoribonuclease, and its mRNAs typically end in a protective stem-loop structure that impedes 3'-exoribonuclease attack, RNA degradation was believed to start with endonucleolytic cleavage at one or more internal sites [4-6]. RNase E, an endonuclease is responsible for such cleavage events and as part of the degradosome cleaves 5' monophosphorylated mRNA and triggers the degradation of the transcripts [7, 8]. The resulting RNA fragments are then degraded by a combination of 3'-exonucleases termed RNase R, PNPase, RNase II and oligoribonucleases [6]. RNase E cleaves RNA within single stranded segments that are AU-rich [9] and although endonuclease cleavage sites can be found at diverse locations throughout RNA transcripts, differences in bacterial mRNA longevity are commonly determined by features of the 5' untranslated region (UTR). Two key features for stabilizing mRNA are a 5'-terminal stem-loop structure and/or a high-affinity ribosome-binding site [2, 10]. In addition, recent studies revealed a mechanism by which 5'-termini govern access of RNase E to internal cleavage sites within primary transcripts [5]. In particular a tri-phosphate at the 5'-end can stabilize transcripts and counteract the activity of RNase E. Removing of the pyrophosphate creates substrates for RNase E. It was shown that the *E. coli* protein RppH can initiate the decay of mRNA by removing the 5'-pyrophosphate *in vitro*. *In vivo* it accelerates the degradation of hundreds of *E. coli* transcripts by modifying their triphosphorylated to a monophosphorylated 5'-end [5], (Fig. 1A).

3.1.1.2. RNA degradation in Gram-positive Bacteria

In *Bacillus subtilis* no orthologue of RNase E has been found. Here, the essential RNase J1 and its paralog RNase J2 have endonucleolytic cleavage specificity similar to RNase E [11]. They also possess a 5'-3' exonuclease activity and prefer monophosphorylated or hydroxylated 5'-ends as substrates. An endonucleolytic cleavage generates a 5'-monophosphate, and the RNA can then be degraded by RNase J1 (5'-to-3') or by 3'-to-5' exonucleases like

RNase R, PNPase and RNase PH. RNase J1, which in addition to its exonuclease activity displays endonuclease activity on some substrates [12] (Fig. 1B), is a member of the metallo- β -lactamases. The protein consists of three domains, the β -lactamase, a β -CASP and a C-terminal domain with the catalytic site located between the β -lactamase core and the β -CASP domain. RNase J combines endo- and exoribonucleolytic activities in a single peptide, and both activities are carried out by the same catalytic site. The enzyme is functional as a dimer and a linker located at the C-terminal domain is required for maintaining its dimeric state [13]. Enzymes of this group are widely distributed in all three kingdoms of life [14].

Moreover RNase Y, an integral part of the degradosome has a large effect on overall mRNA stability in *B. subtilis*. The enzyme is associated with glycolytic enzymes, PNPase and RNase J1/2. It initially performs endonucleolytic cleavage in RNA. The resulting fragments are then degraded by 3'-to- 5' exonucleases [15]. It appears that RNase J1 triggers these initial steps to some extent [16, 17]. Similar to *E. coli*, a 5'-monophosphate increases the activity of these enzymes and a triphosphorylated-5'-terminus constrains decay [13].

3.1.2. RNA degradation in Eukaryotes

In eukaryotic cells mRNAs contain some modifications, which can influence the stability and the degradation process. These include the Cap-structure at the 5'-end, and the poly-(A) tail at the 3'-terminus. The Cap-structure is a 7-methylguanosine Cap with a 5'- 5' triphosphate linkage that stabilizes and protects the mRNA from degradation by 5'-to- 3' exonucleases. In addition shortening of the 3'-poly (A) tail induces decapping of the 5'-end and as a result the transcripts are subjected to 5'-to- 3' directional decay. Decapping does usually not occur until the poly (A) tail is shortened in order to weaken the binding of a decapping inhibitor, termed Pab1p. The translation initiation factor eIF4E plays also an important role in these processes. It binds to the cap structure and influences accessibility, and thereby protects from decapping [18]. Deadenylation and assembly of a complex consisting of seven Lsm (like-Sm) proteins [19], enhances the binding of the decapping enzyme Dcp1p/Dcp2p complex. These Lsm proteins, which contain the "Sm-motif" exhibit a doughnut shape compris-

ing seven identical subunits interacting via β -strand pairing and hydrophobic interactions [20, 21]. The mRNA is then degraded by 5'-to- 3' exoribonucleases such as XRN1 [18], (Fig. 1C).

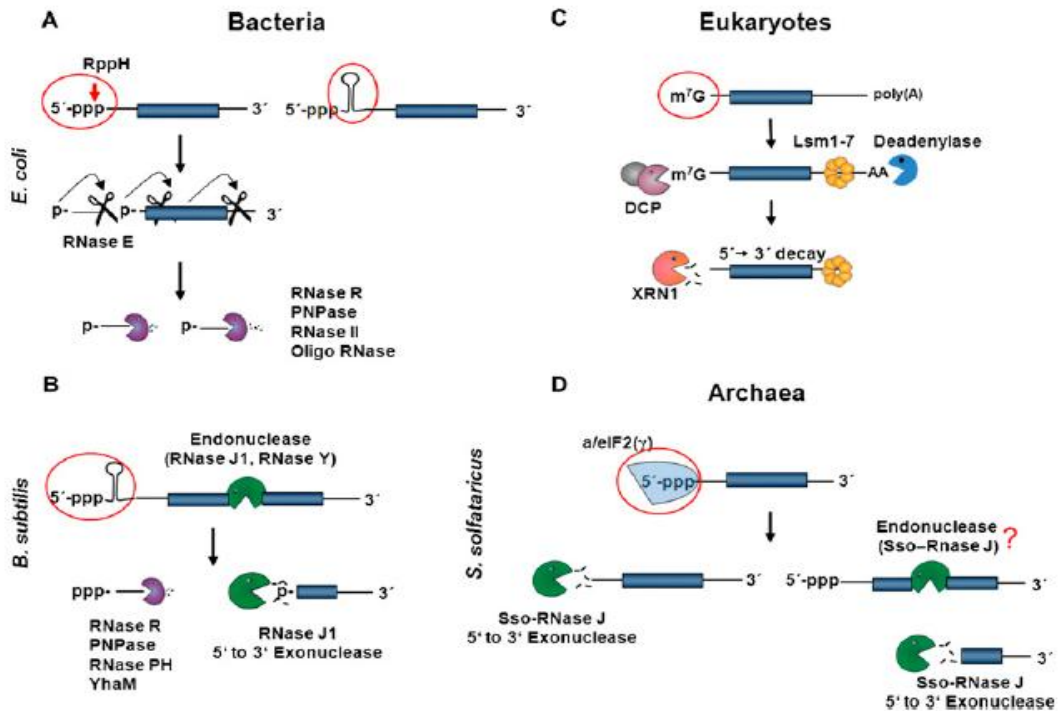


Figure 1. 5'-to-3' directional degradation processes in Bacteria, Eukaryotes and Archaea (A) A 5'-tri-phosphate and/or stem loop structures counteract the activity of RNase E. RppH removes the 5'-pyrophosphate and initiates degradation by RNase E. Endonucleolytic cleavage generates fragments, which are degraded by 3'-to- 5' exonucleases, PNPase, RNase R or RNase II. (B) In *B. subtilis*, endonucleolytic cleavage by RNase J1 and RNase Y initiates decay. The resulting 5'-monophosphate fragments can then be degraded by Rnase J1 (5'-to- 3') and by RNase R, PNPase, RNase PH or YhaM (3'-to-5'). Stem-loop structures can stabilize transcripts. (C) The cap-structure at the 5'-terminus and the 3'-poly (A) tail exert a protective function for eukaryotic mRNAs. Deadenylation and assembling of Lsm1-7 recruit the decapping enzyme complex DCP. The decapped 5'-end is then degraded by a 5'-to-3'exonuclease, XRN1. (D) In the archaeon *Sulfolobus solfataricus* a/eIF2(γ) can bind to the tri-phosphate 5'-end of mRNAs and counteracts Sso-RNase J. Removal of the factor from the triphosphorylated 5'-end is believed to initiate 5'-to- 3' degradation via Sso-RNase J. As an endonucleolytic activity by Sso-RNase J or the presence of other endonucleases cannot be ruled out, it is also possible that endonucleolytic cleavage initiates a 5'-to- 3' degradation [22].

3.1.3. RNA degradation in Archaea

Different RNases with endo- and exonucleolytic activity have been described in the archaeal domain of life [23, 24]. It has become apparent that several as-

pects of the transcriptional processes between Eukaryotes and Archaea are similar [24]. In addition some processes involved in mRNA turnover share similarities. In both, Eukaryotes and Archaea, the exosome emerges as a central 3'-to- 5' RNA processing and degradation machinery. Eukaryotic exosomes comprise RNA-binding proteins, helicases and several 3'-to- 5' exoribuncleases [25, 26]. Proteins of the eukaryotic exosome core subunit were found in most archaeal genomes, including that of *Sulfolobus solfataricus*. The exosome of *S. solfataricus* contains four subunits, which are orthologues of the yeast proteins Rrp4, Rrp41, Rrp42 and Csl4. In addition, a DnaG homologue, which in Bacteria is responsible for synthesizing the RNA primer during DNA-replication is associated with the complex [23]. The complex does not only degrade RNA, but is also able to trim ribosomal RNA substrates. Recent structural studies suggested a model for RNA degradation and trimming by archaeal exosomes (Fig. 2). The 3'-end of transcripts reaches the active site *via* the S1 pore and neck, where the substrates are cleaved. Accessory factors with helicase activity appear to be involved in unfolding of RNA substrates. Sufficiently stable secondary structures do not enter the complex, stop at the S1 pore and thereby impede degradation [27].

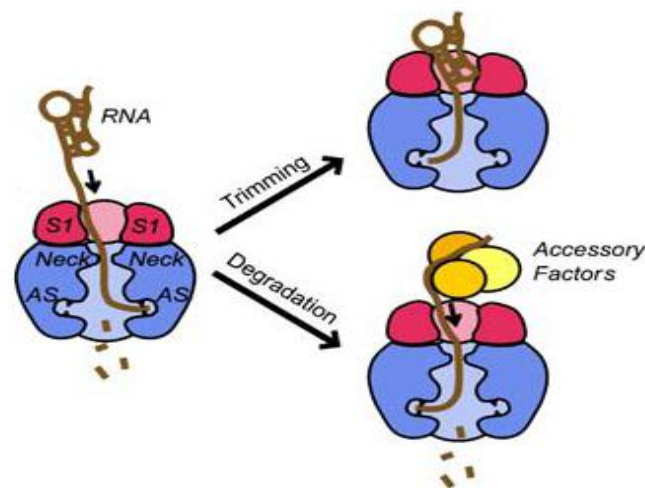


Figure 2. Model for exosome function in Archaea. A single-stranded RNA enters *via* the S1 pore and neck and reaches the active site. It is necessary for degradation that RNA is fully unfolded. Stable secondary structures can stop degradation and cause trimming of the RNA. Accessory factors can unfold transcripts and activate degradation [27].

Archaea do not have bacterial RNase E orthologues, and furthermore there is no evidence that archaeal mRNAs have Cap-like structures, [11]. It was recently demonstrated that the 5'-end of mRNAs is protected from degradation by translation initiation factor *a*/eIF2 in *S. solfataricus* [28]. The trimeric initiation factor *a*/eIF2 consists of three subunits α , β , γ and recruits tRNA_i to the 30S ribosomal subunit. The *a*/eIF2 (γ) subunit was shown to bind to the 5'-end of triphosphorylated mRNA and thereby to counteract 5'-to- 3' decay. Thus, besides its requirement for tRNA_i binding to the ribosome, the initiation factor protects the mRNA from 5'-to- 3' decay (Fig. 1), [22].

3.2. Structure of the RNase J orthologue in *S. solfataricus*

The RNase J orthologue named Sso-RNase J in the crenarchaeum *Sulfolobus solfataricus* was first identified by Hasenöhrl *et.al* [22]. The 492 amino acids long protein has a molecular mass of 55 kDa. The enzyme belongs to the β -CASP family of metallo- β -lactamases and comprises typical signatures such as five β -lactamases and the three β -CASP motifs. This features and the sequence of the protein are highly conserved in the crenarchaeal clade of archaea (Fig. 3) [22].

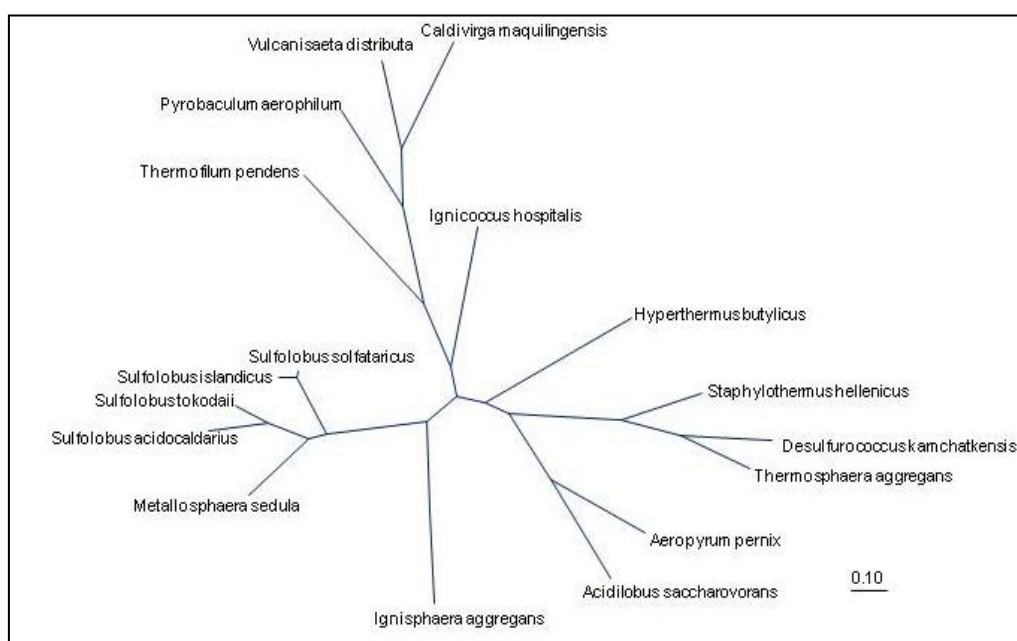


Figure 3. Phylogenetic tree of putative RNase J proteins from the crenarchaeal clade of Archaea. Phylogenetic analyses of putative RNase J

protein sequences were performed with the ARB program package. The bar represents 10% sequence divergence [29]. Although they differ with regard to their substrates, the family of metallo- β -lactamase proteins can be found in all three kingdoms of life. The class B β -lactamases (including glyoxalase II, aryl sulfatases, cAMP phosphodiesterases, etc.) can be distinguished from a separate group with nucleic acid substrates.

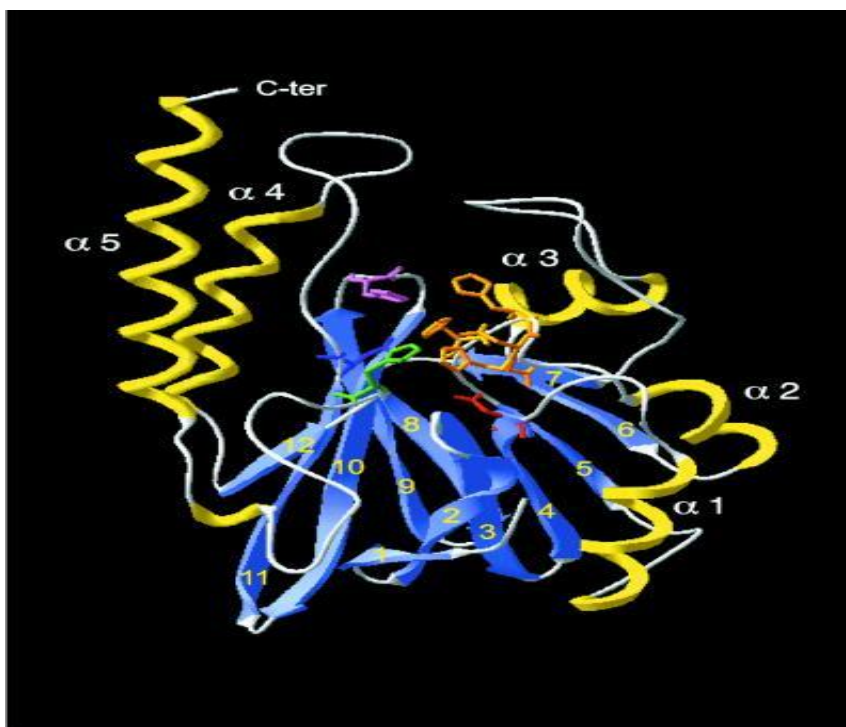


Figure 4. The structure of *Stenotrophomonas maltophilia* metallo- β -lactamase. The strands β 1- β 7 and β 8- β 12 form two β -sheets. The coloured residues are used for binding of zinc [14].

A four-layered β -sandwich with two mixed β -sheets flanked by α -helices and metal-binding sites are structural characteristics of the metallo- β -lactamase fold. Other conserved features in the active enzymes include five motifs consisting of histidines and aspartic acids. A wide shallow groove at the bottom comprises a dinuclear Zn(II) required to perform the cleavage reaction (Fig. 4), [14].

The structure of RNase J of *Thermus thermophilus* was recently determined [30]. The monomer contains three globular domains: the β -lactamase-core, the β -CASP domain and the C-terminal domain. A five-stranded parallel β -sheet surrounded by five α -helices built the β -CASP domain. The domain is located between strand β 12 and helix α 11 in the β -lactamase core (Fig. 5).

RNase J

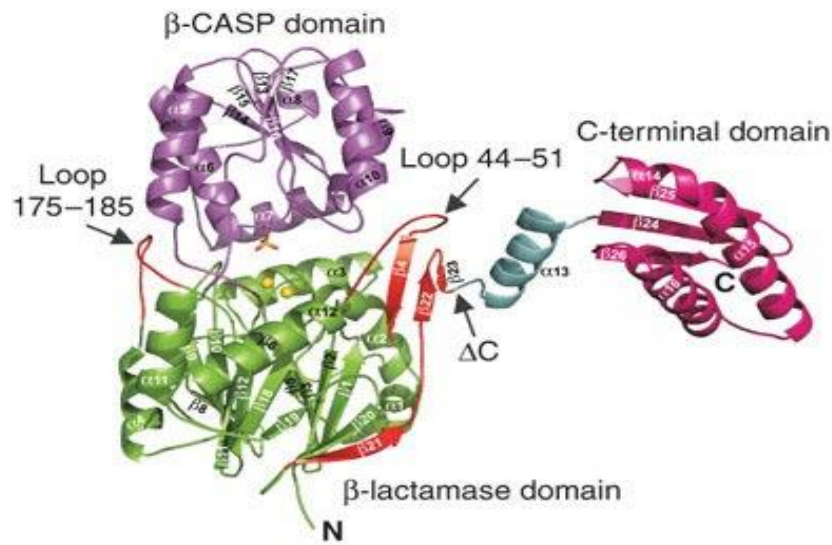


Figure 5. Structure of the RNase J monomer of *T. thermophilus*. The yellow spheres represent the zinc atoms in the active site and the letters N and C indicate the N- and C-terminus, respectively [30]. The C-terminal domain is absent in the *S. solfataricus* orthologue.

When compared to known RNase J proteins Sso-RNase J displays a very low overall sequence similarity. A meta-structure alignment of Sso-RNase J and the known *T. thermophilus* RNase J revealed high structural homologies and identified Sso-RNase J as a RNase J orthologue [22, 31]. This approach reveals structural and functional similarities, undetectable at the primary sequence level. In brief, the meta-structure concept follows the 3D structural information and a calculated network of residue interaction. Based on this network particular residues and edges indicate the existence of neighbourhood relationships. Calculated meta-structure parameters derived from the primary sequence are applied to define pairwise similarity matrices. Thus, the combined bioinformatics search for functional motifs in combination with protein meta-structure analysis offers a powerful tool to identify similar protein functions in the absence of primary sequence homology. However, the Sso-RNase J only shows sequence conservation in the catalytic domain as well as in few other motifs [22]. The C-terminal domain of RNase J, which is essential for activity [30] in *T. thermophilus*, is missing in the archaeal RNase J homologue (Fig. 6).

Tth-J	-----	
Bs-J1	-----	
Pab-J	-----	
SSO0386	MTFVFITVGFSTITIFFSLVSII TLVAFICSVFIPILSIFFRSEGFIFAITCFIEEEVNLIV	61
Tth-J	-----MQDHVEIIPLCGMGEICKMTI VFRFRDEIFVL DGC-----	LAF PREGMP 44
Bs-J1	-----MKFVRNDQTAVFALGCLGEGICKMTI YAVQFQDEIVLIDAG-----	IKF PED ELL 48
Pab-J	-----MMEEINMIKIYTLG-CYE EVGRNMTAV EYNGEVVIV DMCIRLDRLVLIHEDVEFQKMSKD	59
SSO0386	CCYD ISQMNYFLKILGCGREVG RSAIEVGNSDGS ILLDYGVNFDKDNPNFP-----	113
	M1	
Tth-J	GVDLLIP EVDYLI EHRHETKAWVLT HGHEDHICGLPFLLP MIFGKESPVPIYCARLTLGGL	105
Bs-J1	CIDYVIPDYTYLVKRNEDKIKGL FIT HGHEDHICGIPYLLRQVN-----	IPVYCGKLAIGLL 104
Pab-J	LRLGAI PDD RPINRKRVAIALS HGHLDHICGAVCKLAPHYP-----	DVPIYGT PYT IRL 114
SSO0386	-----LQEMPGRVGFVWS HAHLDHICGLPIYQIGSLN-----	TKVYCTVATRIIT 159
	M2	
Tth-J	RGLKEEFGLRPGA FNLKEISPDRIQV-----	GRYFTLDLFRMT HSI PDNSGV 153
Bs-J1	RNKL EHGILL R-QTKLNIICEDDIVKF-----	EKTAVSFFRT HSI PDSYGI 148
Pab-J	AKSEIKGE EYFEVITNP LYE TNYGRIVQV-----	SENLAIEFVQIT HSI PQSSIV 163
SSO0386	ETHLRDF LKL SGAKIPYEWV-EVKITMDNFMAICYGE EVE IDS LRVSLYNAGH-I PGSSII	218
	M3	
Tth-J	VIRTPIGTIVHTGDFKLDPTPIDCKVSHLAKVAQAGAEVLLLIADATNAERPCGYTPSE	EMR 214
Bs-J1	VVKTPPGNIIVHTGDFKDFDTPVCG-EPA NLTKMAEIGKEGVLCLLSDSTNSENPEFTMEERR	208
Pab-J	VVHTPECAVVYACDYKFDNNHPYCE RPDYKRLKELCKEGKVLAE STRVAEETKTPSEAV	224
SSO0386	KVSSKRCVLAFTGDIINLTETKLM---KPAE IENIGDANV LV--MESTYKGFNHPNPKDVE	273
	M4 A	
Tth-J	IAKELDRVI---GRAPGRVFTTFASHIHRIQSVIWA AEKYCKRVAMEGRSMLKFSRIAL	271
Bs-J1	VGES IHD IF---PRVDGRITIFATFASN IHR LQQVIEAAVQNGRKVAVFGRSMESATEICQ	265
Pab-J	AKMLLEDFFLYEGMEADG-LIATTFASHIARLQELIE IANKMGQAIFI GRSLAKTYGIAK	284
SSO0386	NDFYDKV---MEVVESCGTVLVPAF-S-LARSQEVLSVLAERNFPYPVYDGMSEREIT EIM	329
Tth-J	ELGYLRV-KDR-----LYTLEEVKDL PDHQVLILA TCSQCGPMSVLHRLAFEGHAKMAI	324
Bs-J1	TLGYINC PKNT-----FIEHNEINRMPANKVT ILC TCSQCE PMAALSRLANGTHRQ ISI	319
Pab-J	QLCLIRMGGS RVL RSPNAVSKVLKEVVSQARENYL LIVTCHQCEPGA IILT RMANG-ELYDI-	345
SSO0386	LGFKFELNRPDLLKFA YDNFNYVKGWED PHRAMKKEGVIVASA GMLKGGP-AV-----	381
Tth-J	KPGDTVL LSSSPIPGNEEAVNRVINRLYAL-----	GAYVLYPPTYKWHAS CHASQEELK 378
Bs-J1	NPGD TVVFSSSPI PGNTISVSRTINQLYRA-----	GAEVHIGPLNDIHTS CHICGQEEQK 373
Pab-J	GPED TVVFSA CVI PNP LNVAQRYAL ETKLRMK-GVEMIRN-----	IHVSCHASKEDEHR 397
SSO0386	YYFKKLS ENSRNAVFLVSYQAINTPGRK LLEMKKFDREYSCLLKARLEIRDFESSHAGRRQLL	442
	B	
Tth-J	LILNLITPR-FFLPMHCEV EHQMMFNLAE SMS-RPPEKT LIGENGAVYRLTRET FEKVGE	437
Bs-J1	LMLRLIKPK-FMFP HCEYRMQKMHVKLATDCC-IPERNC FIMDNGEVLALKGDEASVAGK	432
Pab-J	YLIRMLNPE-YTVPAHCEP RML THYABLAEE EGYMIGKEV FIS RNCHVVEIPGS-----	448
SSO0386	EIVKSVKDLERKVV LVHGS PDNESSLADLIRQEI---GVEVITPENGQEISL-----	490
	M5/C	
Tth-J	VPHGVLYVDGLGVGDI TEEILADRRHMAEEGLV VITALAGED-----	PVVEVVSRCGFVKAC 493
Bs-J1	IPSGSVYIDGSGIGDI GNIVLRDRRILS EEGLVIVVVSIDMDDFKI SAGPDLISRGFVYMR	494
Pab-J	-----LEG-----	451
SSO0386	-----	
Tth-J	ER--LLGEVRMALEALKNCVREKK-PLERI PDD IYYPVKFLEKATGRDP MILP VVI EG	550
Bs-J1	ESCD LINDAQELI SNHLQKVMERKT TQWSEIKNEITD TLAPFLYKTKRPMILPIMEV	555
Pab-J	-----	
SSO0386	-----	

Figure 6. Alignment of different RNase J orthologues. The blue box contains the N-terminal extension of Sso-RNase J, whereas the β -CASP domain and the C-terminal domain are boxed in black and red, respectively. Yellow marked residues (M1-M5) build up the five β -lactamase motifs and the three β -CASP motifs (A-C) are in green. Purple marks conserved residues, which implicates the formation of the active site of the protein, according to the structure of *T. thermophilus* RNase J. Tth-J = *T. thermophilus* RNase J, Bs-J1 = *B. subtilis* RNase J1, Pab-J = *P. abyssi* RNase J, SSO0386 = *S. solfataricus* Sso-RNase J [22].

3.2.1. Enzymatic properties of Sso-RNase J

The Sso-RNase J was identified as a 5'-to-3' directional exonuclease. Although the enzyme has a preference for 5'-mono- over tri-phosphorylated ends and exerts an accelerated degradation rate of 5'-mono-phosphorylated substrates, there is no evidences for the presence of monophosphorylated mRNA in *S.*

solfataricus [22]. It is currently unknown whether dephosphorylation triggers activation of RNA degradation in these organisms.

The thermophilic archaeon *S. solfataricus* grows between 65°C and 80°C, which agrees with the temperature optimum of Sso-RNase J. Like several other RNA-degrading enzymes e.g. bacterial RNase P or RNase E, Sso-RNase J requires Mg^{+2} for function [22].

As mentioned, in *B. subtilis* an endonucleolytic cleavage induced by RNase J1 or RNase Y triggers the RNA degradation process. Compared to *B. subtilis* RNase J1, which can function as an exo- as well as an endonuclease, the RNase J orthologue in *Sulfolobus solfataricus* appears to display no endonucleolytic activity [22]. However, as the endonucleolytic cleavage of RNase J1 is limited to a few substrates, the possibility exists that Sso-RNase J acts as an endonuclease on certain RNAs. Due to the fact that RNase J1 plays a role in rRNA maturation [12], it cannot be ruled out that Sso-RNase J is also involved in RNA processing.

3.3. a/eIF2 (γ) counteracts 5'-to- 3' mRNA decay

Mechanisms, which protect the 5'-end of mRNAs, have been observed in all three kingdoms of life [12, 18, 32]. In Bacteria stem-loop structures at the 5'-terminus can increase the half-lives of the transcripts [3]. In addition, the phosphorylation status is important for the stability of mRNAs. In *E. coli* the 5'-pyrophosphate has to be removed before degradation can be induced [5]. Eukaryotic mRNAs generally have Cap-structures, which are attached to the 5'-terminus and associated with the Cap-binding complex, which protects the transcripts against 5'-to- 3' directional decay [18] (Fig. 1).

Archaea do not possess a 7-methylguanosine-cap and the high growth temperature impedes the formation of stable stem-loops structures. As mentioned above, the translation initiation factor a/eIF2 binds to the triphosphorylated 5'-terminus of archaeal RNAs and protects transcripts from processing by 5'-to- 3' exonucleases [28]. The archaeal factor a/eIF2 consists of three subunits, α , β and γ . In *S. solfataricus* the smallest subunit is the β -subunit, which consists of 139 amino acids. The α -subunit comprises 266 amino acids, and the γ -subunit, containing a G-domain, is the largest, with a length of

415 amino acids and a molecular mass of 45 kDa. A pivotal function of the factor is to recruit the initiator tRNA (tRNA_i) to the ribosomal subunit. [33]. In the hyperthermophilic archaeon *Pyrococcus abyssi* the tRNA_i binding site seems to reside on the γ -subunit [34], but nevertheless an α - γ dimer is required for a stable interaction with Met-tRNA_i [35]. There are two models for Met-tRNA_i binding in Archaea. One specifies that the α -subunit is not directly involved in the binding process [35] and that the γ -subunit binds tRNA_i through a methionine-binding pocket. In contrast the other model suggests that Met-tRNA_i contacts both the α - and γ -subunit [36]. In addition it has been found that the C-terminal portion of the α -subunit is sufficient for stable tRNA binding [35]. In *S. solfataricus* the a/eIF2 γ -subunit interacts with both α - and β -subunits, whereas the α - and β -subunits do not interact with each other, suggesting that the γ -subunit forms the structural core of the trimeric factor [34].

Studies by Hasenöhrl *et al.* [28] suggested that a/eIF2 binds to the 5' end of mRNA and impedes 5'-to- 3' directional decay. Filter-binding assays revealed that only the γ -subunit is required for binding to the 5'-PPP-terminus of the mRNA. The factor a/eIF2 (γ) does not bind to monophosphorylated or dephosphorylated RNA, respectively. The impediment of 5'-to- 3' directional decay by a/eIF2 (γ) were supported by experiments showing that overproduction of a/eIF2 (γ) resulted in stabilization of mRNA 5'-segments *in vivo* [28]. It was also shown that a/eIF2 (γ) counteracts the activity of Sso-RNase J *in vitro* [22].

Ribosome bound a/eIF2 exhibits an increased affinity for Met-tRNA_i and a decreased affinity for mRNA binding, which agrees with its pivotal function in translational initiation. In Archaea the ribosome levels can vary with grow conditions [37]. It seems conceivable that, under conditions of a feast lifestyle, i.e., when there is a surplus of ribosomes, a/eIF2 fulfills primarily its role in binding Met-tRNA_i and initiates translation. In contrast under famine conditions or during stringent control [38] when the level of ribosomes is low, unbound a/eIF2 (γ) is believed to bind to 5'-triphosphorylated end of mRNAs and to counteract 5'-to-3' decay [28]. Given that, Met-tRNA_i is unlikely to compete for the factor when bound to the triphosphorylated-5'-terminus of mRNAs [28], it poses the question as to the removal of a/eIF2 from 5'-PPP-ends of mRNAs, which would not only

be required for translation of α /eIF2-protected mRNAs, but also for their 5'-to- 3' directional decay.

4. Aims of the study

The RNase J orthologue in *Sulfolobus solfataricus* was identified as the first crenarchaeal 5'-to-3' exonuclease. Its enzymatic properties were studied and the protection from decay by translation initiation factor α /eIF2 via binding to the 5'-triphosphate of RNA was demonstrated. However, the physiological role of Sso-RNase J remained unclear. As it has been reported, that the RNase J1 from *B.subtillis* has endonucleolytic activity on only a few targets [11], Sso-RNase J could also display endonucleolytic activity on some substrates.

Alignment analysis revealed a 70,9 % homology between Sso-RNase J and the RNase J orthologue in *Sulfolobus acidocaldarius* (SacI-RNase J). The β -lactamase and β -CASP motifs as well as the residues implicated in formation of the active side are highly conserved. In this study *S. acidocaldarius* was used as this organism is more amenable to genetic manipulation than *S. solfataricus*. The aim of this study was to unravel a role for SacI-RNase J in RNA metabolism.

5. Materials and Methods

5.1. Bacterial strains and plasmids

All *E. coli* strains were routinely grown in Luria-Bertani broth (LB) [39] at 37°C or 28°C, respectively, supplemented with appropriate antibiotics to maintain the plasmids. 100 µg/ml of ampicillin and 50 µg/ml of kanamycin were added to the medium if required. The archaeal strains were grown in Brock's medium [40] in the presence of 0,2% arabinose and 0,1% N-Z amine or 0,1% tryptone at 75°C. In addition 10 µg/ml uracil was added. The pH was adjusted to 2-3 with sulfuric acid. The bacterial/archaeal strains, plasmids and media used in this study are listed in Table 1.

Table 1. Bacterial strains and plasmids used in this study

<i>Sulfolobus</i> strain	Genotype	Source
<i>Sulfolobus acidocaldarius</i> MW001	<i>pyER⁻, lacS</i>	Albers <i>et al.</i> 2011, unpublished
<i>Sulfolobus acidocaldarius</i> MW001Δ2362	<i>pyER⁺, lacS, Δ2362</i> (gene, encoding for SacI-RNase J is knockout in this strain)	This study
<i>E. coli</i> strain	Genotype	Source
TOP 10	F- <i>mcrAD (mrrhsdRMSm crBC) φ80lacX74 nupG recA1 araD139 Δ(ara-leu) 7697galE15galK16rpsL (Str^R)</i>	Invitrogen
BL21 (Rosetta)	F ⁻ , <i>dcm, ompT, hsdS(rB-mB-), galλ(DE3)</i>	Stratagene
<i>E. coli</i> ER1821	F ⁻ <i>glnV44 e14(McrA⁻) rfbD1? relA1? endA1 spoT1? thi-1 Δ(mcrC-mrr) 114::IS10</i>	New England Bio Labs _{INC.}
Plasmid	Description	Source
pEt-28b	T7 promoter, His-tag coding sequence, MCS, <i>lacI</i> coding sequence, (Kan ^R)	Novagen
pET28b-Saci_2362	<i>Saci_2362</i> (gene coding for SacI-RNase J with C-terminal His-tag),	This study (5.2.1.)
pΔ2pyrEF	pBluescript-based vector with <i>S. solfataricus pyrEF</i> gene	[41]

Saci_2362 deletion plasmid	p Δ 2pyrEF-Vector containing Saci_2362 deletion cassette	(Albers <i>et al.</i> 2011 unpublished results)
pEt28b-Sacl_a/eIF2 (y)	Sacl-a/eIF2 (y) with N-terminal His-tag	(Hasenöhrl <i>et al.</i> 2010 unpublished results)
pEt28b-Sso_a/eIF2 (y)	Sso-a/eIF2 (y) with N-terminal His-tag	[33]

LB-Medium (1l)

NaCl	10 g
Yeast Extract	5 g
Pepton	10 g
For plates	15 g/l agar

Brock's-Medium (50ml)

1000x Brock solution (8.1.)	50 μ l
200xBrock solution (8.1.)	250 μ l
100xBrock solution (8.1.)	500 μ l
H ₂ SO ₄ (50%) → pH should be 2 to 3	17,5 μ l
If required :	
20% N-Z Amine	500 μ l
Uracil (10mg/ml)	50 μ l
20% D(-)-Arabinose	500 μ l
10% Lactose	2 ml

Table 2. Used oligonucleotides

Primer	Sequence	Properties	Genome coordinates
A72_FP	5'-TTCTTCCATGGCTAT GGATTCAGTGAAGTACT GGGC-3'	Saci_2362 forward primer, cleavage site for NcoI (underlined)	Start: 2209571 End: 2209596
B72_RP	5'-AAGAACTCGAGTAG GTTAATCTCCTTACCGT TTCCG-3'	Saci_2362 reverse primer, cleavage site for XhoI (underlined)	Start: 2210807 End: 2210832
2508fl_FP:	5'-AGATAATACGACTC ACTATAGATGATTGTA GGATTTGCCGAAAA ACT-3'	Sso_2508 forward primer (full length 2508 RNA)	Start: 2276631 End: 2276657
2508fl_RP:	5'-TCATTTTCGCTCA CCCATACTAAAGTTACA CT-3'	Sso_2508 reverse primer (full length 2508 RNA)	Start: 2277742 End: 2277774
2508fl_5'	5'-CTTTCTCTAGTTTT TATTAGTTTTCCGG CAAATCCTAC-3'	Complementary to the 5'-end of 2508fl-mRNA	Start: 2276638 End: 2276677
2508fl_central	5'-ACATCTTCGACTG TAATAGATTTCTGAACA GAGCTTTAGG-3'	Complementary to the central part of 2508fl-mRNA	Start: 2277166 End: 2277206

2508fl_3'	5'-CGCTCACCCAA TACTAAAGTTACACTGT GC CTTCTA-3'	Complementary to the 3'-end of 2508fl- mRNA	Start: 2277732 End: 2277767
40A1- oligonucleo- tide (5'-end)	5'-AGACAGAAACCAC AGAACGAGACAGAAA CCACAGAACGTCCTATA GTGAGTCGTATTAC-3'	Designed as sub- strate for RNase J assays (labeled on 5'-end	----
3'-end oligo- nucleotide	5'-GTCAGAAACCA CAGAACG AGACAGAAACC ACAGAACGACCTATA GTGAGTCGTATTAC-3'	Designed as sub- strate for RNase J assays (labeled on 3'-end	----
T7-oligo	5'-GGGCTCTAGAGTA ATACGACTCACTATA GG-3'	Containing a T7- promoter for in vitro transcription	----
Saci_2362_ KO_Fw_up_ PstI	5'-GTACTGCAGCTTCG ACCCTTCTCGTAATC-3'	upstream flanking region, forward pri- mer, cleavage site for <i>PstI</i> (underlined)	Start: 2208701 End: 2208720
Saci_2362_KO _Rv_up	5'-GAAGAATTATCATT AATTCAACCGCCAAAC- 3'	upstream flanking region, reverse primer	Start: 2209550 End: 2209569
Saci_2362_ KO_Fw_dwn	5'-CGGTTGAATTAAT GATAATTCTTCTAATTC- 3'	downstream flanking region, forward primer	Start: 2209556 End:2 210850
Sa- ci_2362_KO_R v_dwn_ <i>Bam</i>HI	5'-GATGGATCCTGCG TCCTGTAGGTAATCAC- 3'	downstream flanking region, reverse pri- mer, cleavage site for <i>Bam</i> HI (underlined)	Start: 2211682 End: 2211701
KO_test RP	5'-CTACGAAGGGTAT CCATTCC-3'	Primers annealing on <i>Saci_2362</i> flanking down-regions	Start: 2211788 End: 2211807
KO_test FP	5'-AGGAAGCATTAAG GTGTAAC-3'	Primers annealing on <i>Saci_2362</i> flanking up-regions	Start: 2208586 End: 2208605
test_PCR_Saci RP1	5'-CTGTAAATCAGTG CTGTTACAAT-3'	testing chromosomal DNA	Start: 1516600 End: 1516622
test_PCR_Saci FP1	5'-GGAGGCTCATT GGTCGAATCCA-3'	testing chromosomal DNA	Start: 1517148 End: 1517169
test_PCR_Saci RP2	5'-AGTCGGGATTCC AGTCTGAAATG-3'	testing chromosomal DNA	Start: 1618994 End: 1619016
test_PCR_Saci FP2	5'-CCATCTGTTC AAT TCTCTGCTA-3'	testing chromosomal DNA	Start: 1619801 End: 1619823

5.2. Construction of plasmids

5.2.1. pET-28b (*Saci_2362*)

The gene *Saci_2362* encoding the enzyme SacI-RNase J was amplified by means of PCR using genomic DNA from *Sulfolobus acidocaldarius* as template. The forward primer A72_FP: 5'-TTCTTCCATGGCTATGGATTCAAGTGAAGATACTGGGC-3' and the reverse primer B72_RP: 5'-AAGAACTCGAGTAGGTTAATCTCCTTACCGTTTTCCG-3' were used for PCR amplification. The underlined sequences contain restriction sites (*Nco*I, *Xho*I) for insertion into the corresponding sites of plasmid pET-28b (Novagen). The recombinant vector pET28b-*Saci_2362* was sequenced and transformed into *E.coli* BL21 (Stratagene). The oligonucleotides used are listed in Table 2.

5.3. Purification of SacI-RNase J and α /eIF2 (γ)

The gene coding for SacI-RNase J (*Saci_2362*) was cloned into the expression vector pET28b (Novagen) and the plasmid was transformed into *E. coli* BL21 (Stratagene).

Expression of *Saci_2362* was induced for 3h at 37°C with 1 mM IPTG when cells reached an OD₆₀₀ of 0,5. The cells were lysed by addition of lysozyme and sonication and the lysate was centrifuged at 10,000 g for 10 minutes. Recombinant RNase J containing a C-terminal His-tag was purified to homogeneity under denaturing conditions (8M urea) by affinity chromatography on Ni-NTA agarose following standard protocols (QIAGEN) (8.1.). To remove urea, the sample was dialyzed against different buffers (100 mM KCl, 50 mM Tris-HCl, pH=7 containing 4M, 2M, 1M or 0M urea, respectively) starting with the highest concentration of urea. In addition, the sample was diluted 1:5 with d_4 H₂O (to a total volume of 10 ml) before dialysis, to avoid aggregation of the protein. The sample was concentrated to 1/10 of the volume by using a centrifugation filter unit (MILIPORE™) with a cutoff at 3 kDa. The purified protein was stored at -80°C in the presence of 5% glycerol.

The α /eIF2 γ -subunit from *S. solfataricus* and *S. acidocaldarius*, respectively was prepared as described before [33]. 1l of *E.coli* BL21 harboring the

recombinant plasmid pEt28b-SSo_a/eIF (γ) or pEt28b-Saci_a/eIF2 (γ) were incubated at 37°C until it reached an OD₆₀₀ of 0.5. The synthesis of a/eIF2 (γ) was induced for 3h by addition of 1 mM IPTG. The cells were lysed and the cell extracts were heated for 10 minutes at 70°C, and then centrifuged at 10,000 g for another 10 minutes to precipitate heat-labile *E. coli* proteins. The recombinant aIF2 (γ), which contained an N-terminal tag of six histidines, was purified by affinity chromatography on Ni-NTA agarose following standard protocols (QIAGEN) under native conditions. The bound protein was eluted with buffer containing increasing concentrations of imidazol (1.fraction: 100% Wash-buffer; 2.fraction: 80%Wash-buffer + 20% Elution-buffer; 3.fraction: 60% Wash-buffer + 40% Elution-buffer; 4.fraction: 40% Wash-buffer + 60%Elution- buffer; 5.fraction: 20% Wash-buffer + 80% Elution-buffer; 6.fraction: 100% Elution-buffer; 8.1.). The purified proteins were dialyzed against storage buffer (100 mM KCl, 10 mM Hepes and 5% glycerol) and aliquots were stored at -80°C. All buffers and solution for purification are listed in 8.1.

5.4. Preparation of RNA substrates

40A1 RNA

To characterize the enzymatic properties of SacI-RNase J, two different, 42-nt-long, synthetic RNAs (5'-PPP-40A1 RNA and PPP-40A1-3' RNA), both with a tri-phosphate group at the 5'-end (PPP) were used in the assays (5.7.). Both RNAs harbored a single radioactive labeled A nucleotide at the 5'end or at the 3'end. The 5'-labeled and 3'-labeled RNA, respectively were synthesized as follows: The nucleotide 5'-GGGCTCTAGAGTAATACGACTCACTATAGG-3' containing a T7-promoter was hybridized to a second oligonucleotide, either the 40A1-oligonucleotide (5'-AGACAGAAACCCACAGAACGAGACAGAAACCAAGAACGTCCTATAGTGAGTCGTATTAC-3') or the 3'-end oligonucleotide (5'-GTCAGAAACCCACAGAACGAGACAGAAACCCACAGAACGACCTATAGTGAGTCGTATTAC-3'), by heating to 90°C and followed by cooling at 37°C. The duplex (Fig. 7) was used as template for *in vitro* transcription using the Ambion MEGAshortscript T7 Kit together with radioactive [α -³²P]ATP. The reaction mix is listed in 8.1. Subsequently, the RNA was loaded on a polyacrylamide (12%)

gel containing 8M urea and purified by standard gel extraction, yielding the respective RNA radioactively labeled at the 5'-end and 3'-end, respectively. The oligonucleotides used are listed in Table 2.

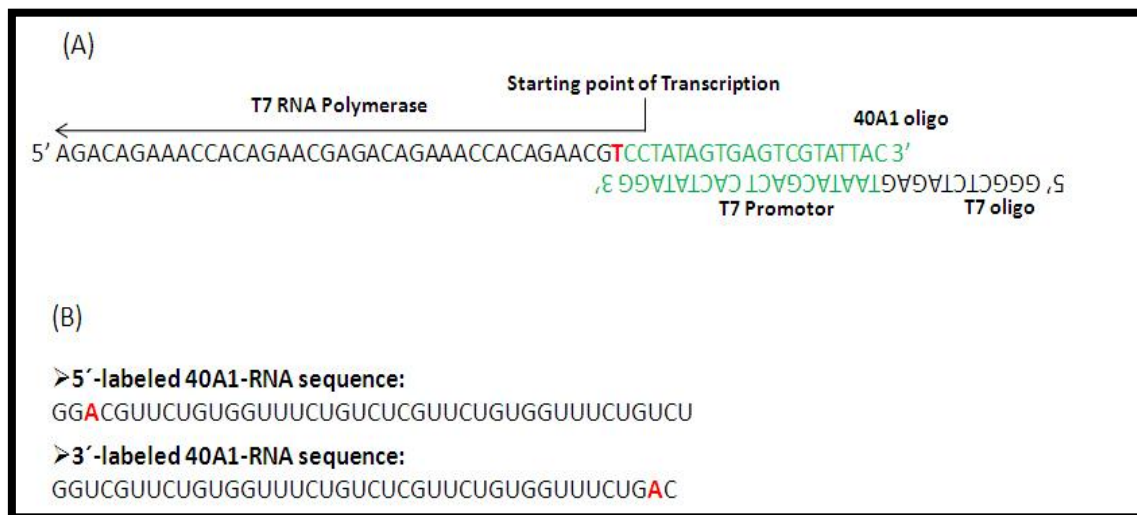


Figure 7. *In vitro* transcription of 5'-PPP-40A1 and PPP-40A1-3'. (A) The T7 oligo was hybridized to the 40A1 oligo and this construct was used as the template for *in vitro* transcription. (B) The resulting RNAs harbor either a single radioactive labeled A nucleotide at the 5'-end or at the 3'-end, respectively.

2508fl RNA

For testing RNase activity in *SacI*-extracts (5.7.) 2508 full-length (2508fl) RNA transcribed from the gene *SSO_2508* was prepared. 2508fl DNA oligonucleotide was amplified by means of PCR from genomic DNA isolated from *S. solfataricus* M16, using the primers 2508fl_FP: 5'-AGATAATACGACTCACTATAGA TGATTGTAGGATTTGCCGGAAGAACT-3' and 2508fl_RP: 5'-TCATTTTCGCT CACCCATACTAAAGTTACACT-3' (Tab. 2). The PCR yielded the template for *in vitro* transcription, using the Ambion MEGashortscript T7 Kit (8.1.). After *in vitro* transcription, the RNA was purified with phenol/CHCl₃ standard purification (8.2.).

5.5. Labeling of DNA oligonucleotides

For Northernblot analysis (5.8.) 2508fl_5'-, 2509fl_3'- and 2509fl_central-oligonucleotides were labeled with [³²P]. The oligonucleotides are listed in Table 2. The reaction mix, containing DNase-free ddH₂O, the respective oligonucleo-

tides (10 pmol/μl), [γ - 32 P]ATP, T4 Polynucleotide Kinase (PNK) and reaction buffer (Fermentas) (8.1.) was incubated at 37°C for 45', and then incubated at 65°C for 10'. Afterwards the radioactively labeled oligonucleotides were purified with Nucleotide Removal Kit (QUIAGEN) and stored at -20°C

5.6. Enzyme assays with SacI-RNase J

The assays were conducted as previously described [22]. RNase J activity was assayed in a 10 μl reaction volume containing 10 mM MgCl₂, 10 mM KCl, 5 mM Tris, 0,25 μM of the respective RNA substrate (5.4.) and 500 ng of purified SacI-RNase J (5.3.). The reaction mix was incubated for 0 to 60 min at 65°C. The reaction was terminated by addition of RNA-loading dye, containing 0,025 % SDS and 0,05 mM EDTA and incubated on ice. Subsequently, the samples were loaded on a 20 % PAA / 7M urea gel. The gel was subjected to autoradiography using a Typhoon 8600 PhosphorImager.

5.7. Test for RNase activity in SacI-extract

Cell extracts from *Sulfolobus acidocaldarius* MW001 and MW001Δ2362 were prepared as described [42]. The strains were grown in Brock's medium at 75°C to an OD₆₀₀ of 0,4. 200 ml of culture were pelleted by centrifugation at 4000 rpm for 10 min at 4°C and resuspended in buffer A (20 mM Tris/HCl pH=7.4; 10 mM Mg-Acetate; 50 mM NH₄Cl; 1 mM DTT). Lysozyme was added and the cells were sonicated for 3 minutes. Then, the samples were centrifuged at 30.000 g for 60 min and the supernatant (S30 extract) was stored at -80°C.

The S30 extracts, were preincubated for 1h at 70°C to degrade most of the endogenous RNAs. 2508fl RNA (0,25 μM) was added to the samples, and incubation was continued for 0–90 min at 70°C. The reaction mix contained 0,25 μM of 2508fl RNA, 10 mM MgCl₂, 20 mM Tris pH 6.5, 10 mM KCl, and either cell extract from MW001 or the mutant strain MW001Δ2362. The protein concentration of the extracts was determined spectrophotometrically with a Thermo Scientific NanoDrop 2000 and the samples were adjusted to a final concentration of 0,25 μg protein extracts/μl. The total volumes of the samples were 120 μl. Aliquots (20 μl) were removed after 0, 10, 30, 60 and 90 min. The

reaction was stopped by adding 1 µl of 0.5 M EDTA and 20 µl RNA loading dye followed by cooling on ice.

To follow degradation of 2508fl RNA after addition of *Saci*-extracts (5.7.) a Northern-blot with labeled oligos (2508fl_5', 2508fl_central and 2508fl_3' listed in Table 2) was performed. The prepared samples were transferred to a membrane (Amersham HybondTM, GE healthcare.) by using a filtration apparatus (Minifold® II, Schleicher & Schuell BioScience). The membrane was exposed to UV-light for 20 sec to cross-link RNA and then pre-incubated with hybridization solution Rothi®-Hybri-Quick at 45°C for 1h. Afterwards, the labeled oligonucleotides ((2508fl_5', 2508fl_central and 2508fl_3') were added and incubated o/n at 45°C. The membrane was washed with washing-solution I (200 ml SSC [20x], 10 ml 20% SDS), washing-solution II (10 ml SSC [20x], 10 ml 20% SDS) (8.1.) and ddH₂O for 10 min and air-dried. The membrane was subjected to autoradiography using a Typhoon 8600 PhosphorImager.

5.9. Construction of the *S. acidocaldarius* Δ2362 (*Saci*-RNase J) deletion mutant

5.9.1. Construction of the *Saci*_2362 deletion plasmid

For the construction of the *Saci*_2362 deletion plasmid, the respective up- (868 bp) and downstream (2145 bp) flanking regions of *Saci*_2362 were PCR amplified from *S. acidocaldarius* genomic DNA. To amplify the upstream region the primers *Saci*_2362_KO_Fw_up_ *Pst*I: 5'-GTACTGCAGCTTCGACCCTTCTCGTAATC-3' and *Saci*_2362_KO_Rv_up: 5'-GAAGAATTATCATTAATTCAACCGCCAAAC-3' were used. For the amplification of the downstream region the primers *Saci*_2362_KO_Fw_dwn: 5'-CGGTTGAATTAATGATAATTCTTCTAATTC-3' and *Saci*_2362_KO_Rv_dwn_ *Bam*HI: 5'-GATGGATCCTGCGTCCTGTAGGTAATCAC-3' were used. By overlap extension PCR the up- and downstream flanking regions were joined by using the outward bound primer of the respective primer pair. Overlap extension PCR represents an approach in which complementary oligonucleotides and the polymerase chain reaction are used to generate two DNA fragments having overlapping ends. These fragments are combined in a subsequent 'fusion' reaction in which the overlapping ends an-

neal, allowing the 3' overlap of each strand to serve as a primer for the 3' extension of the complementary strand. The resulting fusion product is amplified further by PCR [43]. The overlap extension PCR products were cleaved with *Pst*I and *Bam*HI and subsequently ligated into plasmid p Δ 2*pyr*EF, which contained the *pyr*EF cassette from *S. solfataricus* [41]. This ligation yielded the *Saci_2362* deletion plasmid. The plasmids, strains and primers used are listed in Table 1 and Table 2, respectively.

5.9.2. Construction of the *S. acidocaldarius* MW001 Δ 2362 deletion mutant

The *Saci_2362* deletion plasmid was transformed into competent *E. coli* ER1821 cells (8.2.). After incubation for 1 hour at 37 °C, the cells were transferred to 4 ml LB medium containing ampicillin/ kanamycin. The cultures were incubated overnight at 37 °C with shaking (190 rpm). The plasmid was purified using GeneJET™ Plasmid Miniprep Kit. The *Saci_2362* deletion plasmid was transformed into *S. acidocaldarius* MW001 via electroporation as described in [44]. 50 μ l of electro-competent *S. acidocaldarius* MW001 cells were mixed with 100 ng or 300 ng of plasmid. The mixture was transferred to 0.1 cm electroporation cuvettes (Bio-rad). The electroporation program was set as follows: 1500 Volt, 600 Ω and 25 μ F. A Genepulser MXcell, Bio-rad electroporator was used. After electroporation the cells were mixed with 50 μ l of 2x Brock's medium and incubated for 30 minutes with shaking at 350 rpm. The tubes were aerated by opening the lid every 10 minutes. After incubation, the cells were seeded first on selection gelrite plates without uracil (8.2) and incubated at 75°C for 5 to 6 days. The deletion mutant *S. acidocaldarius* MW001 Δ 2362 was confirmed by sequencing obtained PCR products using the primers KO_test FP and KO_test RP. All used primers are listed in Table 2.

5.10. High-throughput-sequencing

To identify possible mRNA targets of *SacI*-RNase J, the transcriptomes of *S. acidocaldarius* MW001 and MW001 Δ 2362 which contains a lesion in *Saci_2362* (*SacI*-RNase J) were analyzed by deep sequencing. The high-throughput sequencing of cDNA is an approach, in which the resulting sequence reads are individually mapped to the source genome and counted to obtain the number

and density of reads corresponding to RNA from each known gene [45]. The respective strains (MW001 and MW001 Δ 2362) were grown in Brock's medium supplemented with 0,1% tryptone and 10 μ g/ml uracil. For each transcriptome analysis, total RNA from cultures in logarithmic phase of growth ($OD_{600}\approx 0,35$) and in stationary phase of growth ($OD_{600}\approx 0,75$) were prepared as follows: Total RNA was isolated, using Trizol as described in [46] (8.2.). Afterwards the samples were treated with DNase I (DNase I recombinant, RNase-free, Roche Applied Science) and a control PCR was performed to confirm complete degradation of chromosomal DNA. The used primers (test_PCR_RP1/2, FP1/2) are listed in Table 2. The RNA was fragmented to an average length of 200 nt by incubation for 2 minutes at 94°C in 40 mM Tris-acetate pH 8.2, 100 mM potassium-acetate and 30 mM magnesium-acetate [45]. Subsequently, the samples were cooled on ice and purified over a Sephadex G50 column. The cDNA synthesis was conducted using the Invitrogen cDNA synthesis Kit. 1 μ g of total RNA was mixed with 1 μ l random hexamers primers (100pmol/ μ l, PROMEGA) and DEPC- ddH_2O , to a total volume of 10 μ l. The mixture was heated to 70°C for 10 min and incubated on ice. 4 μ l of first strand reaction buffer (Invitrogen cDNA synthesis Kit), 2 μ l of 0,1M DTT and 1 μ l of 10 mM dNTP were added and incubated at 45°C for 2 min to equilibrate the temperature. Afterwards 1 μ l SuperScriptTM II RT was added and the mixture was incubated at 45°C for 1h. To terminate the reaction the sample was placed on ice. Then, the following reagents were added: 91 μ l DEPC- ddH_2O , 30 μ l second strand reaction buffer (Invitrogen cDNA synthesis Kit), 3 μ l 10 mM dNTP, 1 μ l *E. coli* DNA ligase (10 U/ μ l), 4 μ l *E.coli* DNA polymerase I (10 U/ μ l) and 4 μ l *E. coli* RNase H (2 U/ μ l), to a final volume of 250 μ l. This mixture was incubated for 2h at 16°C. After 2h, 2 μ l of T4 DNA polymerase (10 U/ μ l) were added and incubation at 16°C was continued for 5 minutes. The sample was incubated on ice and 10 μ l of 0,5M EDTA was added. The cDNA was purified with phenol/ $CHCl_3$ as described in 8.2.

6. Results

6.1. SacI-RNase J

6.1.1. Purification of SacI-RNase J

High level synthesis of recombinant proteins in *E. coli* can lead to the formation of insoluble aggregates. To avoid the formation of inclusion bodies, the protein SacI-RNase J was purified under denaturing conditions, using 8M urea. These conditions solubilize inclusion bodies and 6xHis-tagged proteins (QIAexpressionist™). If the pH is reduced to 5.3-4.5, the histidine residues of the His-tag, fused to RNase J are protonated and the recombinant protein can be eluted.

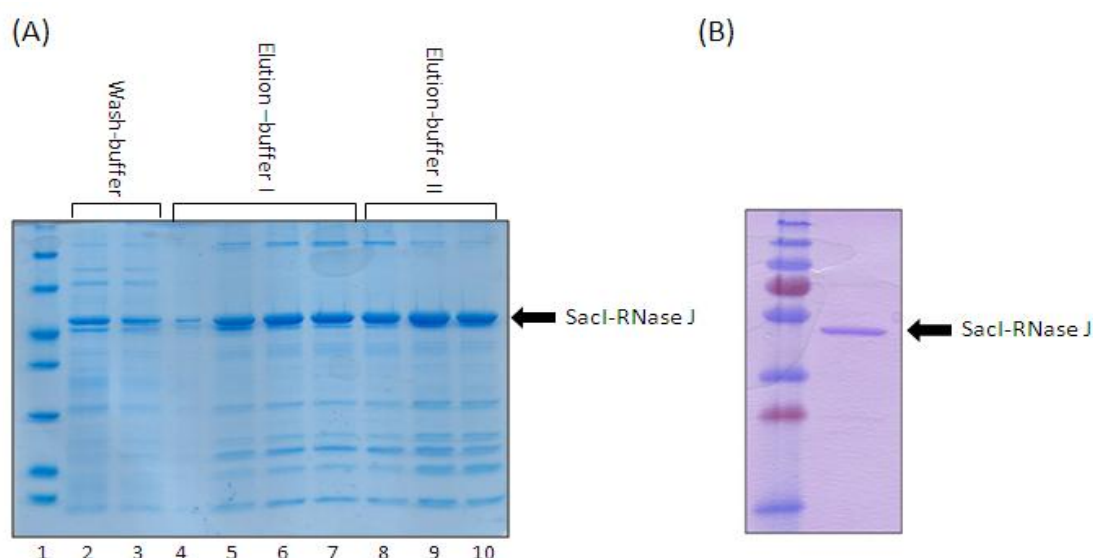


Figure 8. Purification of SacI-RNase J. (A) The protein was eluted by using buffers with different pH-values. The samples were separated by 12% SDS-polyacrylamide gel electrophoresis and stained with FERMENTAS Pageblue™. Lanes 2 and 3, elution with washing-buffer at pH 6.3. lanes 4-7 elution with elution-buffer I at pH 5.9 and lanes 8-10 elution with elution buffer II at pH 4.5. The samples from lanes 5-10 were pooled and used for further purification. (B) The pooled samples were dialysed against storage buffer 100 mM KCl, 50 mM Tris-HCl pH 7. Afterwards, the sample was incubated at 65°C to precipitate non heat-stable *E.coli* proteins, on a 12% SDS-polyacrylamide gel which was stained with FERMENTAS Pageblue™.

The eluted fractions were loaded on a SDS-polyacrylamide gel and the samples containing SacI-RNase J were pooled and used for further purification (Fig. 8A). As SacI-RNase J was purified under denaturing conditions, it was step-wise

renatured by removing urea (5.3.). SacI-RNase J was further purified by heating to 65°C in order to precipitate mesophilic *E. coli* proteins (Fig. 8B).

6.1.2. Enzymatic properties of SacI-RNase J

To characterize the enzymatic properties of SacI-RNase J, a series of assays were conducted (5.6.). A 42-nt-long synthetic RNA (termed 5'-PPP-40A1) harboring a tri-phosphate group at the 5'-end and a single radioactively labeled A nucleotide at the 5'-terminus was used to assess the anticipated 5'-to- 3' directional activity of the recombinant SacI-RNase J. Degradation of 5'-PPP-40A1 RNA was only observed in the presence of Sac-RNase J, whereas in the absence of the enzyme the RNA remained stable (Fig. 9A). The RNase J orthologue in *S. solfataricus* has a temperature optimum of 65°C [22]. To test whether the SacI-RNase J activity depends on the temperature the reaction mix was incubated on 37°C and 65°C, respectively. As shown in Figure 9B, a higher activity was observed at 65°C.

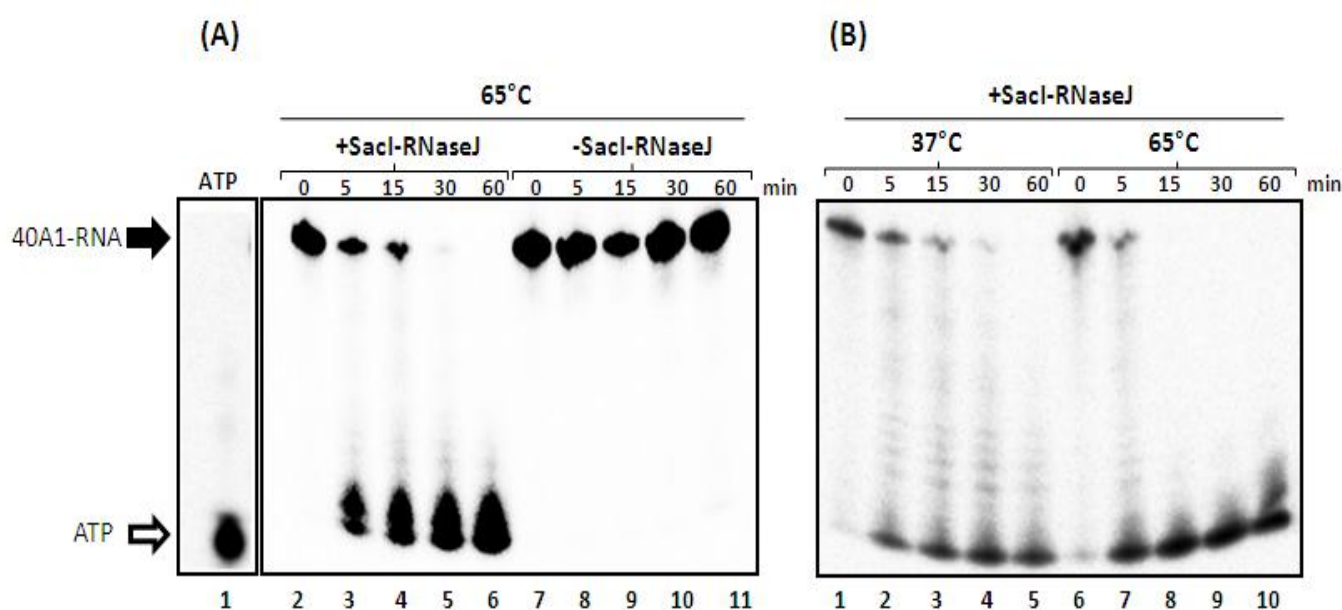


Figure 9. (A) SacI-RNase J displays nuclease activity. [α - 32 P]ATP was loaded on the gel (lane1). 5'-PPP-40A1 labeled RNA was incubated for 0' to 60' at 65°C in the presence (500 ng) (lane 2-6) and in the absence of SacI-RNase J (lane 7-11). (B) The reaction mix was incubated at different temperatures; 37°C (lane1-5) and 65°C (lane 6-10).

Several RNA-degrading enzymes, like bacterial RNase P, RNase H [8] or SSo-RNase J [22] require Mg^{+2} for activity. 5'-PPP-40A1 RNA was therefore incubated with SacI-RNase J in the presence and absence of Mg^{+2} . As shown in

Figure 10, the activity of the enzyme depends on Mg^{+2} , confirming that SacI-RNase J, has similar enzymatic properties as its orthologue in *S. solfataricus* [22].

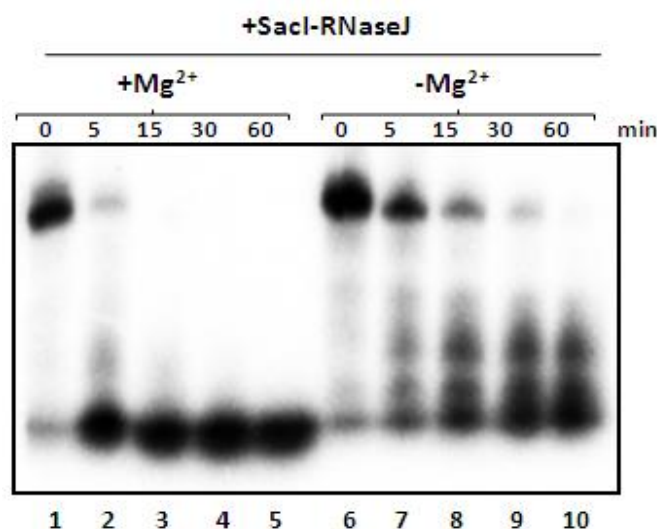


Figure 10. SacI-RNase J and 5'-PPP-40A1 was incubated with (10 mM) (lane 1-5) and without Mg^{+2} (lane 6-10) for 0' to 60' at 65°C.

6.1.3. SacI-RNase J displays 5'-to- 3' exonuclease activity

Next, we addressed the question whether SacI-RNase J displays endo- or exonucleolytic activity and attempted to determine the directionality of the RNase activity. 5' end labeled (5'-PPP-40A1) RNA and a RNA radioactively labeled at the 3'-end (termed PPP-40A1-3') were used as substrates. As shown in Figure 11 (lanes 2-6), the addition of SacI-RNase J to 5'-PPP-40A1 RNA resulted in a single nucleotide as a final degradation product, indicating an exo- rather than an endo-nucleolytic activity. The degradation pattern of the 3'-end-labeled PPP-40A1-3' RNA showed a "smear" and several bands (Fig. 11, lanes 7-11). In contrast the 5'-PPP-40A1 RNA showed only the final degradation product i.e. a single nucleotide, indicating a 5'-to-3' directional decay. Taken together, the results suggested that SacI-RNase J functions as a 5'-to- 3' exonuclease, which is depended on Mg^{+2} .

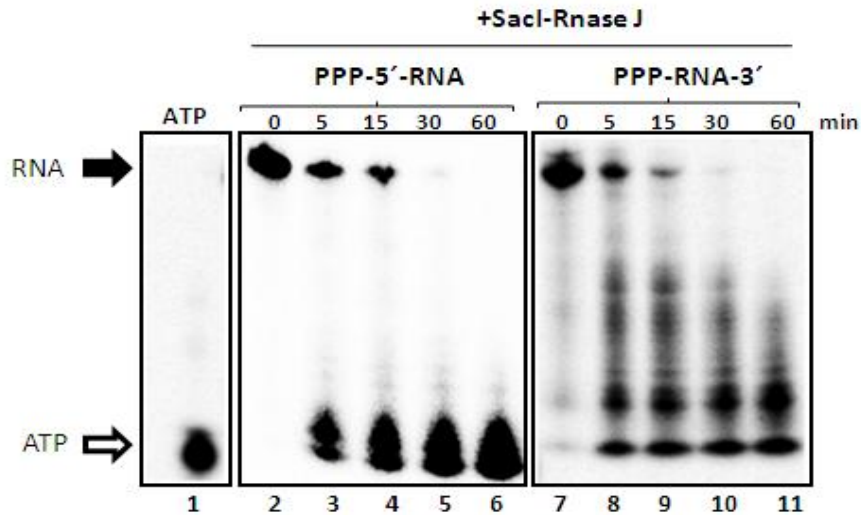


Figure 11. Two different substrates 5'-PPP-40A1 and PPP-40A1-3' were used in this assay. The 5'-end labeled RNA (lane 2-6) and the 3'-end labeled RNA (lane 7-11) shows different degradation pattern. The reaction mix was incubated for 0' to 60' at 65°C.

6.3. Protection of the RNA 5'-terminus by a/eIF2 (γ)

In Bacteria and Eukaryotes, the 5'-end of mRNAs is protected by secondary structures and by the Cap complex, respectively [2, 6, 18]. It was recently shown that translational initiation factor a/eIF2 of *S. solfataricus* binds *via* its γ -subunit to the 5'-tri-phosphorylated terminus of RNA and thereby impeded a 5'-to- 3' directional mRNA decay *in vitro* and *in vivo* [28]. Previously studies showed that the Sacl-a/eIF2 (γ) has the same binding affinity for the 5'-triphosphate of RNA as its counterpart in *S. solfataricus* (D. Hasenöhrl, unpublished data). Thus, we anticipated that Sacl-a/eIF2 displays the same protection activity as Sso-a/eIF2. In order to confirm protection of the 5'-terminus of RNA by Sacl-a/eIF2 (γ), 5'-PPP-40A1 RNA was used, and its decay by Sacl-RNase J was monitored in the presence and absence of the γ -subunit. As shown in Figure 12, when a/eIF2 (γ) was preincubated with 5'-PPP-40A1, i.e. pre-bound to the 5'-end of the RNA, a lower rate of 5'-to- 3' directional decay was observed in the presence of a/eIF2 (γ) indicating protection of the RNA.

The translational initiation factor a/eIF2 (γ) binds to tri-phosphate-5'-termini [28]. Hence, these results confirmed the 5'-end-dependend activity of Sacl-RNase J and the protective function of a/eIF2 (γ).

(A) α /eIF2 (γ) from *S. solfataricus*

(B) α /eIF2 (γ) from *S. acidocaldarius*

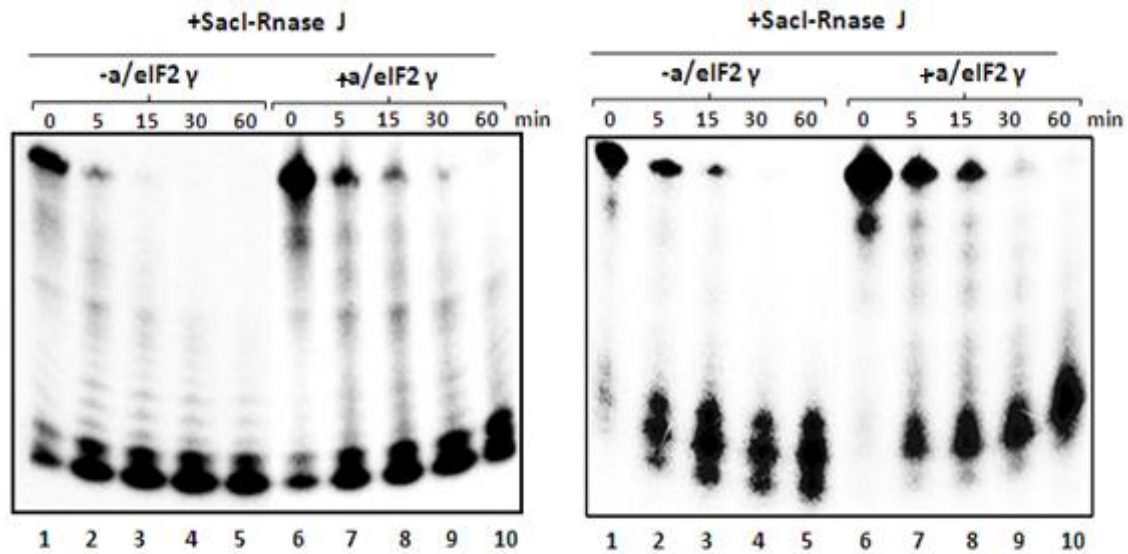


Figure 12. The α /eIF2 (γ) impedes RNA from degradation by counteracting SacI-RNase J. (A) 5'-PPP-40A1 RNA (5 pmol) was incubated for 0 to 60 minutes at 65°C in the presence of SacI-RNase J, without (lane 1-5) and with (lanes 6-10) of pre-bound SSo- α /eIF2 (γ) (25 pmol). (B) This experiment was performed with the γ -subunit from *S. acidocaldarius* SacI- α /eIF2 (γ) (lanes 1-5 absence of SacI- α /eIF2- γ -subunit; lanes 6-10 presence of SacI- α /eIF2- γ -subunit).

6.4. Characterization of the *S. acidocaldarius* Δ 2362 (RNase J) deletion strain

The deletion of the gene *Saci_2362*, encoding for the SacI-RNase J in *S. acidocaldarius* was performed as described in 5.10. [47]. First the growth behavior of the wildtype MW001 and the deletion strain, termed MW001 Δ 2362 was compared by measuring the OD₆₀₀ over a period of 8 days. There were no significant differences, although the knockout strains grew marginally faster and reached a slightly higher OD₆₀₀ in stationary phase (Fig. 13).

Next, it was tested whether the presence or absence of SacI-RNase J in *S. acidocaldarius* affects the stability of the model RNA 2508fl. Total protein extracts from *S. acidocaldarius* MW001 and MW001 Δ 2362 (Tab. 1) were prepared (8.2.) and degradation of the model RNA 2508fl (5.4.) was monitored by Northern-blot analysis (5.8.). Radioactively labeled DNA oligonucleotides, complementary to the 5'-end, to the central part and to the 3'-terminus of 2508fl RNA were used to determine the decay of mRNA (Tab. 2).

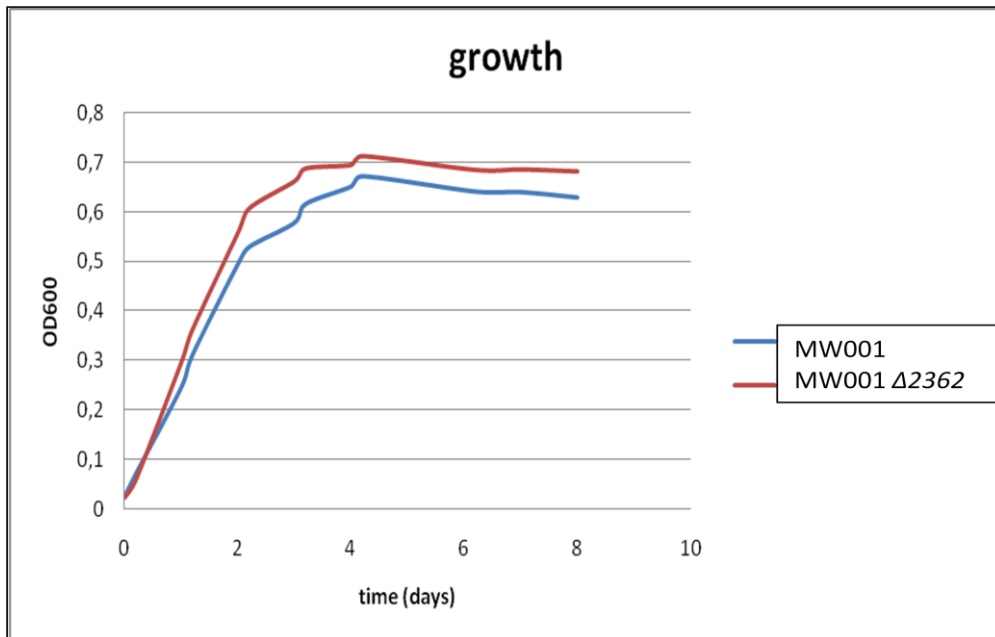


Figure 13. Growth curve of *wildtype* MW001 and MW001 Δ 2362. The cultures were grown at 75°C in Brock's medium supplemented with 0,1% tryptone and 10 μ g/ml uracil. The pH was adjusted to 2.5 with sulfuric acid. The OD₆₀₀ was measured over a period of 8 days.

Compared to the results obtained with the MW001 extracts, 5'-to- 3' degradation of the 2508fl RNA was reduced, with the MW001 Δ 2362 extract. Interestingly, the decay at the 3'-end as well as at the central part of 2508fl RNA was decreased, indicating that the absence of SacI-RNase J stabilizes mRNA (Fig. 14B).

(A)

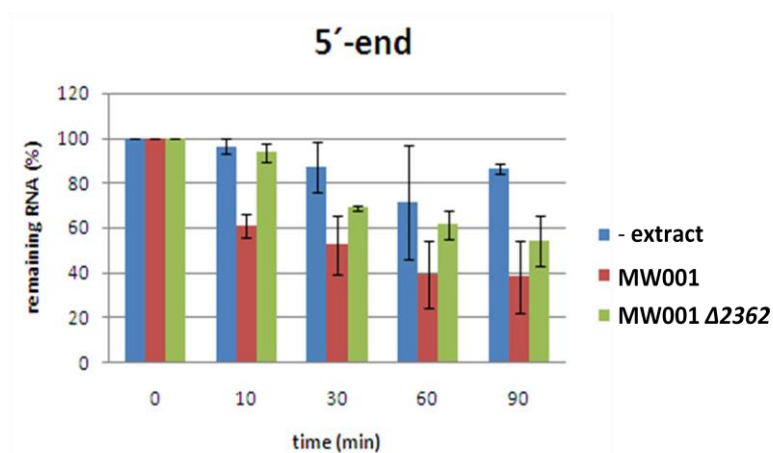


Figure 14 (A). The signals for the 5'-end degradation were quantified with ImageQuant software. Signals at time 0 were set to 100%. The bars show the amount of remaining RNA. The values are an average of three independent experiments. Blue = - extract; red = MW001, green = MW001 Δ 2362

(B)

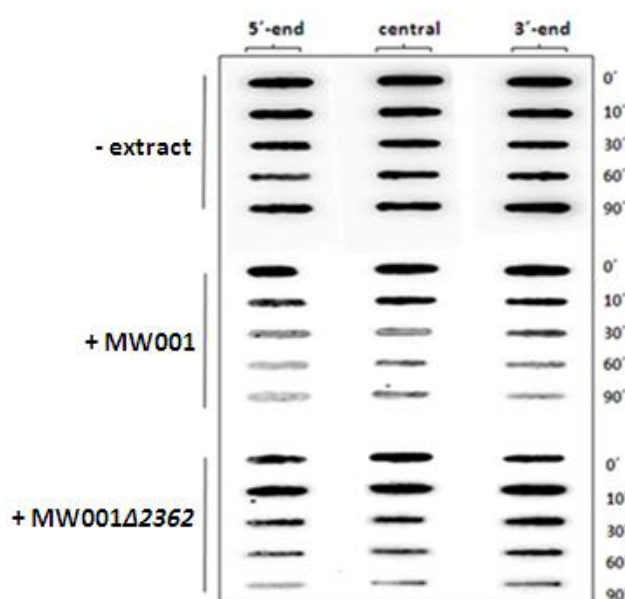


Figure 14 (B). Degradation of 2508fl RNA by total-protein extracts from MW001 and MW001 Δ 2362, respectively. Radioactively labeled oligonucleotides complementary to the 5'-end, the central part and to the 3'-end were used for the Northern-blot analysis (Tab. 2). The samples were incubated for 0 to 90 minutes at 65°C. The 5'-end signals were visualized by autoradiography using a Typhoon 8600 PhosphorImager (Fig 14A).

6.4. 1 Differentially expressed genes in *S. acidocaldarius* MW001 and MW001 Δ 2362

To reveal potential target RNAs of SacI-RNase J *in vivo*, the transcriptomes of MW001 and MW001 Δ 2362 were analyzed in exponential and in stationary growth phase by next generation RNA sequencing (NGS; Illumina platform GAllx). For each transcriptome analysis randomly primed cDNA was prepared (5.10.) from 1 μ g of total RNA fragmented to 200-300 nucleotides. The fragmentation of the RNA reduces secondary structures, which may shield transcripts from priming during cDNA synthesis [45]. The obtained reads were mapped onto the genome of *Sulfolobus acidocaldarius*, using Segemehl [59] (Fig. 15).

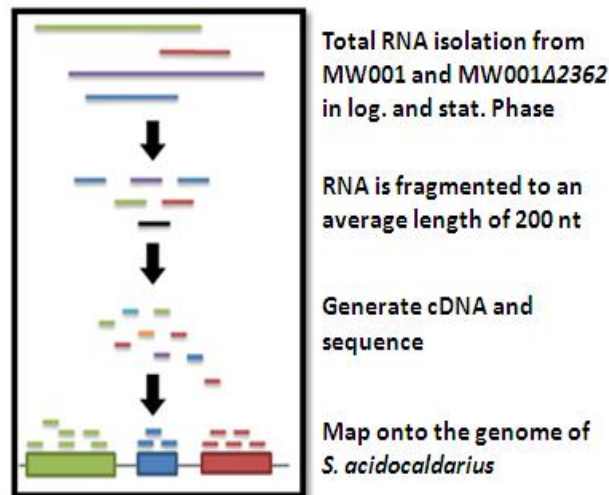


Figure 15. Outline of the RNA-Seq procedure. Total RNA was isolated from wildtype MW001 and MW001Δ2362. The RNA was fragmented to an average length of 200 nt by magnesium-catalyzed hydrolysis and then converted into cDNA by random priming. The cDNA was sequenced and the obtained reads were mapped onto the genome of *S. acidocaldarius*.

First, we addressed the question whether *Saci_2362* mRNA (encoding SacI-RNase J) is predominantly transcribed in logarithmic or in stationary phase. The quantification of the reads suggested, that the level of the *Saci_2362* transcript is higher during exponential growth when compared with stationary phase (Fig. 16). In the mutant strain MW001Δ2362, *Saci_2362* mRNA was not detected, which confirmed the deletion of the *Saci_2362* gene.

The reads mapping to un-annotated regions (according to NCBI data base) were used to predict new transcripts. Segments of the genome were classified as being transcribed, using a sliding windows approach, i.e. every window with a length of 15 nt, which had a higher (median + mean)/2 read coverage when compared with the complete genome, was classified as being transcribed. In a second step, these windows were clustered together into transcribed units (reads that either overlap or were less than 10 nt apart). Most of them showed an overlap with an already annotated gene (NCBI data base) and were discarded from further analysis. The remaining 3150 loci were examined for the potential to encode ncRNAs, using RfamScan and RNAz [48, 49], as well as for a potential ORF. RNAz combines comparative sequence analysis and structure prediction, and can identify conserved RNA secondary structure in multiple sequence alignments. The approach consists of two basic components

(i) a measure for RNA secondary conservation based on computing a consensus secondary structure, and (ii) a measure for thermodynamic stability, which is normalized with respect to both sequence length and base composition [48]. The Rfam database was used in combination with INFERNAL [49] to annotate RNAs in genomes, using consensus RNA profiles to search nucleic acid sequence databases for homologous RNAs or to create new sequence- and structure-based multiple sequence alignments. 112 genes were finally classified as ncRNA candidates (104 by RNAz and 8 by RfamScan) and were further included for the comparison of the transcriptomes of MW001 and MW001 Δ 2362, whereas the remaining loci (3038) were omitted. In addition 67 genes containing a potential ORF were found, but since they were not annotated in the NCBI database and were not conserved in other crenarchaeota species (*S. solfataricus* P2, *S. tokodaii* str. 7, *Metallosphaera sedula* DSM 5348, *S. acidocaldarius* DSM639) these genes were not included in further analysis.

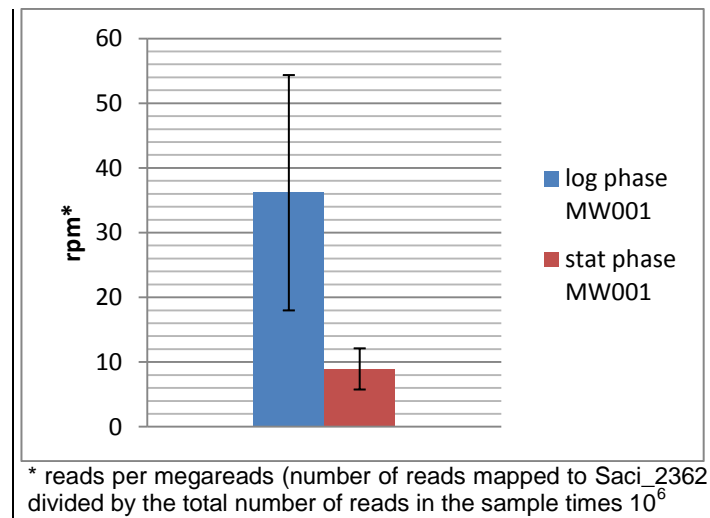


Figure 16. Abundance of Saci_2362 mRNA in MW001 in log. phase and in stat. phase, respectively. The values are an average of two independent sequenced samples.

Next, we determined which transcripts are more abundant in the mutant strain (= potential targets of SacI-RNase J) when compared with the wildtype strain. For this purpose DEseq [50] was used to compare the transcriptomes of MW001 and MW001 Δ 2362 during logarithmic growth and in stationary phase, respectively.

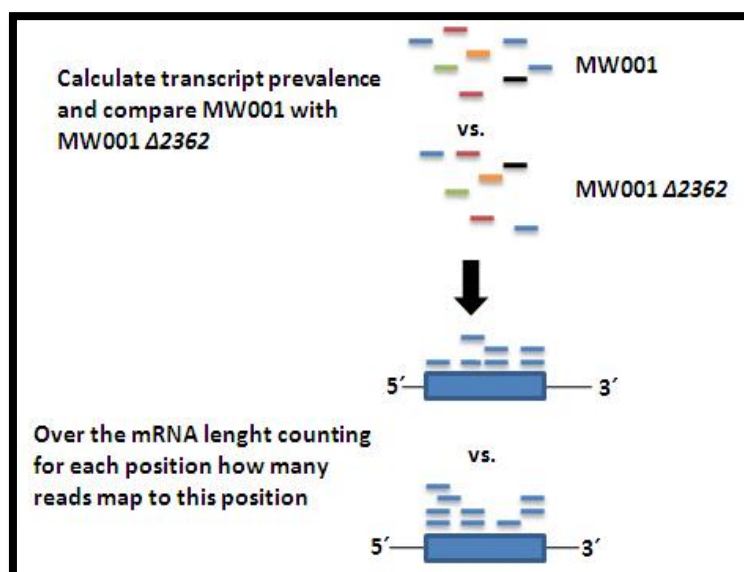


Figure 17. DESeq [50] was used to compare the transcriptomes of MW001 and MW001 Δ 2362. Transcripts, which show different expression levels were further analyzed by counting the reads for each position.

All genes, annotated in NCBI (National Center for Biotechnology Information) and the 112 candidate ncRNAs, were included in the DESeq analyses. Figure 18 shows the log₂ fold change versus the mean expression for all analyzed genes.

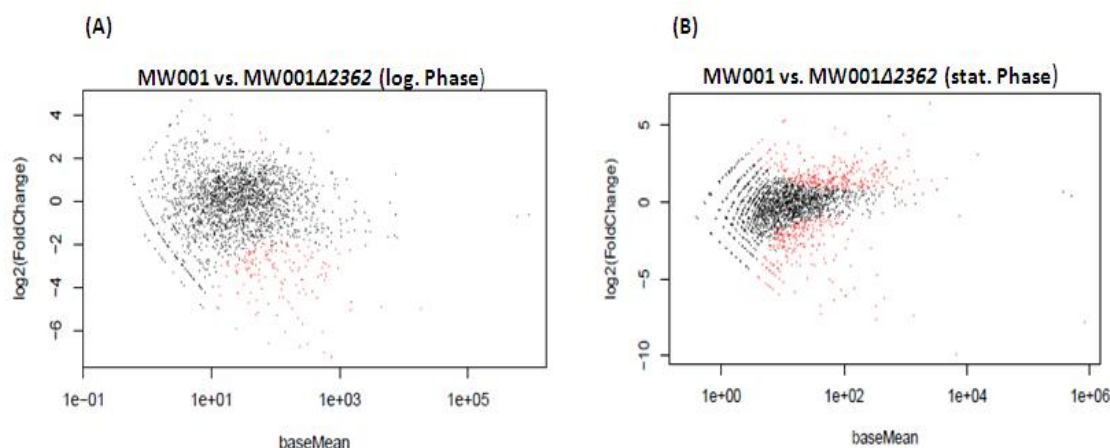


Figure.18. DESeq analysis of MW001 versus MW001 Δ 2362 (A). The log₂ fold change shows the different abundance of transcripts in MW001 and in MW001 Δ 2362 in logarithmic growth phase (each dot represents one transcript). (B) Differentially abundant transcripts in MW001 and MW001 Δ 2362 in stationary phase of growth. Red dots represent transcripts which are differentially abundant in both strains.

When compared with strain MW001, 171 genes and 496 genes were differentially regulated in MW001 Δ 2362 in logarithmic growth phase and during stationary phase, respectively. The corresponding genes were included in further

bioinformatic analyses. As, SacI-RNase J was identified as a 5' → 3' exonuclease we made attempts to identify transcripts degraded at the 5'-end. The reads mapping to different positions in the corresponding mRNAs were assessed and normalized to the total read count. The coverage of reads in each transcript was determined and the differences between the wildtype and mutant were plotted. The differences of the coverage of the 5'-end are represented by the slope of a calculated regression line. One selected plot is shown in Figure 19. When compared to a given transcript isolated from MW001Δ2362 a decreased number of “5'-end-reads” in a corresponding transcript from MW001, give rise to a positive slope of the regression line. In other words, it was assessed whether the 5'-region of a given transcripts is more abundant in the mutant, and therefore probably predominantly degraded in a 5' → 3' direction.

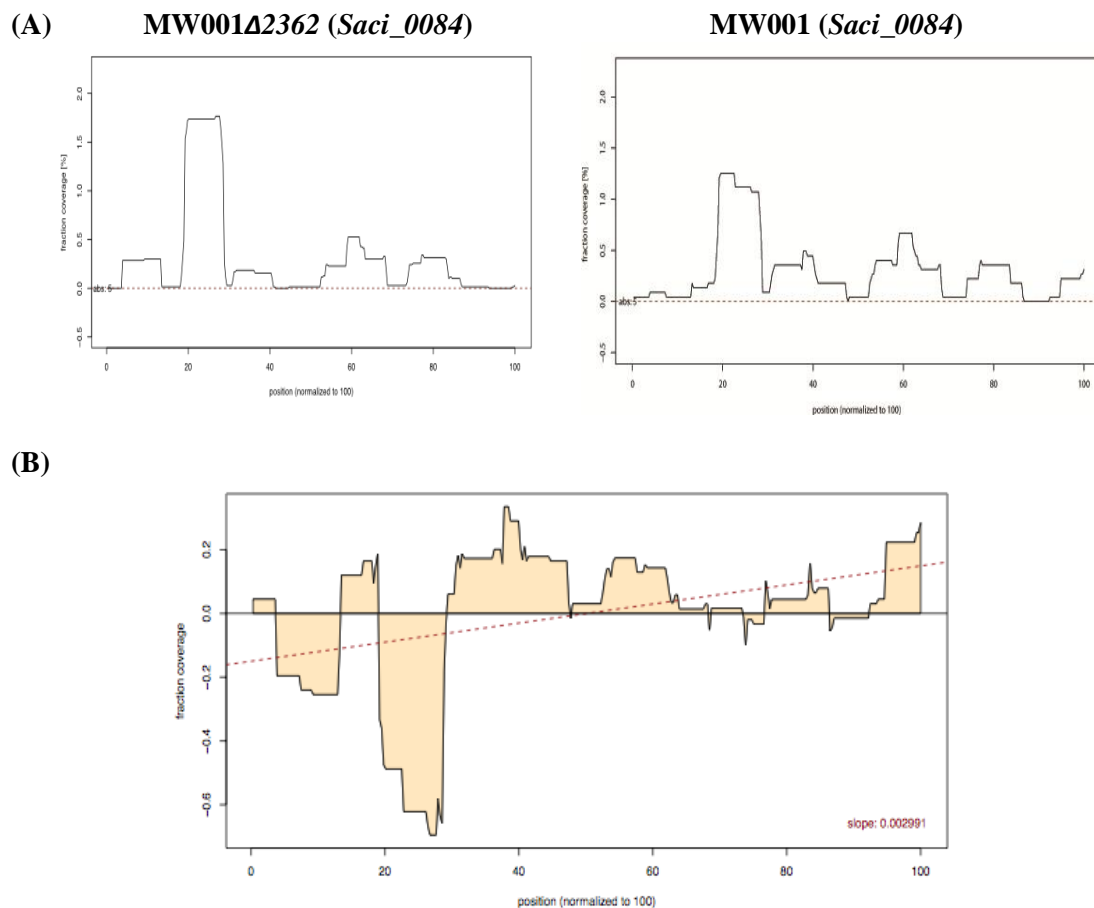


Figure 19. Read distribution over *Saci_0084*. (A) Individual reads mapped to a certain position in the RNA were counted in MW001Δ2362 and MW001. The length of the transcript was normalized to 100 beginning with the 5'-end (x-axis). The fraction coverage gives the number of counts to each position [%] (go to 0 on y-axis). (B) “MW001 coverage” minus “MW001Δ2362 coverage” was plotted and a regression line was calculated. The slope of this regression line represents the differences of the coverage of

the 5'-end. Preferential degradation from the 5'-end of the RNA corresponds, to a positive slope of the regression line.

In the next step, only transcripts were selected, which were more abundant in the mutant strain (\log_2 fold change \geq mean plus the standard deviation) and which showed in addition a positive slope of the regression line (above the mean plus the standard deviation). The p-value (calculated from DEseq, [50]) cut-off was set to 0,1. As potential targets of SacI-RNase J, 13 and 14 transcripts emerged during growth in stationary and in logarithmic phase, respectively (Tab 3).

logarithmic phase (14 counts)		stationary phase (13 counts)	
Gene number	Annotated function	Gene number	Annotated function
Saci_0084	50S ribosomal protein	Saci_0158	Short chain dehydrogenase
Saci_0401	Cobalamin biosynthesis protein CbiG	Saci_0211	Hypothetical protein
Saci_0582	30S ribosomal protein 58P	Saci_0384	Hypothetical protein
Saci_0595	50S ribosomal protein L23	Saci_0673	Hypothetical protein
Saci_0696	Nucleoside diphosphate kinase	Saci_0730	Hypothetical protein
Saci_0708	5-formaminoimidazol-4-carboxamide-1-(beta)-D-ribofuranosyl 5'-monophosphate synthase like protein	Saci_0892	Hypothetical protein
Saci_1119	Hypothetical protein	Saci_1212	Hypothetical protein
Saci_1386	Hypothetical protein	Saci_1515	Hypothetical protein
Saci_1410	Hypothetical protein	Saci_1821	DNA protection protein DPS
Saci_1524	Hypothetical protein	Saci_1832	Hypothetical protein
Saci_1551	Hypothetical protein	Saci_2086	4.5 kDa protein
Saci_1705	dTDP-4-dehydrohamnose reductase	Saci_2197	Hypothetical protein
Saci_2153	Acetyltransferase	Saci_2309	Hypothetical protein
Saci_2158	Hypothetical protein		

Table 3. Potential targets of RNase J (Gene numbers and annotated function according to the UCSC genome browser, <http://archaea.ucsc.edu/cgi-bin/hgGateway?db=sulfAcid1>). These 27 ORFs fulfilled the following criteria, i.e. (i) the \log_2 fold change is \geq mean plus the standard deviation, (ii) the slope of the regression line is \geq mean plus the standard deviation.

and *T. thermophilus*, but it displays sequence conservation in the putative catalytic domain (Fig. 21).

Motif 2									
H	S	H	L	D	H	V	G	S	<i>S. acidocaldarius</i>
H	A	H	L	D	H	I	G	A	<i>S. solfataricus</i>
H	G	H	E	D	H	I	G	G	<i>T. thermophilus</i>
H	G	H	L	D	H	I	G	A	<i>P. abyssi</i>
H	G	H	E	D	H	I	G	G	<i>B. subtilis</i>
H		H		D	H		G		

Figure 21. Motif 2 present in the catalytic domain of RNase J in *T. thermophilus*, is conserved in Sso-RNase J and SacI-RNase J [22].

A notable difference is that the C-terminal domain, which is essential for function in Bacteria is missing in the RNase J homologues derived from *S. solfataricus* and *S. acidocaldarius*.

We have characterized the SacI-RNase J as a 5'-to- 3' directional exonuclease and revealed the similarities to its counterpart in *S. solfataricus*. Like Sso-RNase J, SacI-RNase J requires Mg^{+2} for function (Fig. 12). No hints were obtained for an endonucleolytic activity of SacI-RNase J using 5'-end-labeled synthetic RNAs. RNase J1 in *B. subtilis* has a dual activity, acting as an exo- and an endonuclease, but the endonuclease cleavage of RNase J1 is limited to a few substrates [11, 12]. Thus, we cannot exclude endonuclease activity of SacI-RNase J on certain mRNA targets.

Protection of the 5'-end of mRNAs occurs in all three kingdoms of life. In Bacteria the phosphorylation status of the 5'-end and stem-loop structures at 5'-ends, affect the stability of transcripts [5, 51]. In contrast to Bacteria, eukaryotic mRNAs possess a 7-methylguanosine Cap attached to the triphosphate-5'-end which protects against 5'-to- 3' degradation [52]. In *S. sulfolobus* the γ -subunit of translational initiation factor a/eIF2 was shown to bind to the 5'-end and to impede a 5'-to- 3' directional decay. The Sso-a/eIF2 (γ) shows high simi-

larity with the subunit of *S. acidocaldarius*, and the alignment revealed a high homology of the protein sequences (Fig. 22). Therefore, it was not surprising to find the same binding affinity of Sso-a/eIF2 (γ) and SacI-a/eIF2 (γ) to RNA *in vitro* (Hasenöhrl, unpublished data). Herein, we have demonstrated that SacI-a/eIF2 (γ) counteracts the activity of SacI-RNase J and slows down 5'-to-3' directional decay of RNA (Fig. 14). Considering the prevalence of leaderless mRNAs in *Sulfolobus* [53], 5'-end protection by the γ -subunit might be relevant. These mRNAs start directly with or only a few nucleotides upstream of the start codon, and therefore could be preferred targets of 5'-to-3' exoribonucleases, like Sso-RNase J or SacI-RNase J, respectively.

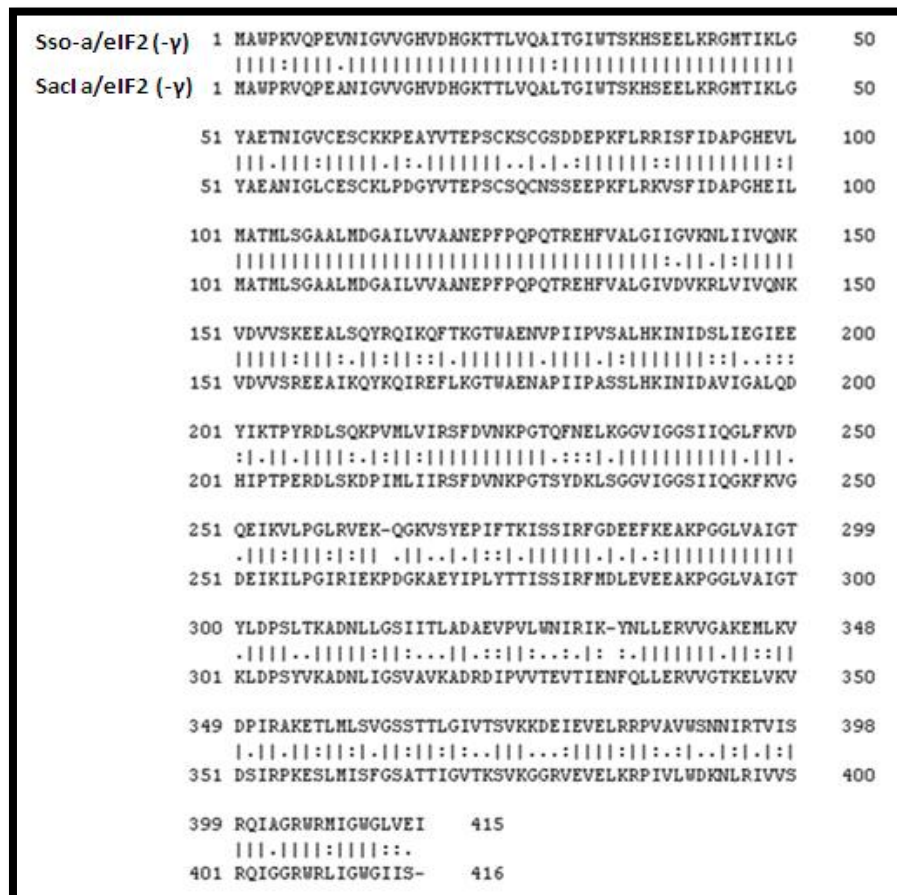


Figure 22. Alignment of Sso-a/eIF2 (γ) from *S. solfataricus* and SacI-a/eIF2 (γ) from *S. acidocaldarius*, using ClustaW2. Sso-a/eIF2 (γ) and SacI-a/eIF2 (γ) display an 85,4 % overall homology.

To assess the biological relevance of SacI-RNase J in *S. acidocaldarius*, the transcriptomes of MW001 and MW001 Δ 2362 were analyzed by high throughput RNA sequencing. We detected 667 RNAs, whose abundances were significant-

ly altered in the mutant strain when compared to the wildtype. These included 496 and 171 transcripts differentially regulated in stationary phase and exponential phase, respectively. In addition, we observed that the RNase J knockout strain reached a slightly higher OD₆₀₀ in stationary phase than the wildtype (Fig. 15). Surprisingly, the abundance of the *Saci_2362* mRNA was higher in logarithmic phase than in stationary phase (Fig. 16), which cannot be easily reconciled with the higher number of transcripts differentially regulated in stationary phase. However, it is known that *B. subtilis* RNase J1 is produced in significant excess over the cell's need [54, 55]. Considering this, the detected amount of *Saci_2362* mRNA may not reflect the actual amount of active protein in the cells.

For potential targets of RNase J a decreased abundance of respective transcript was expected in MW001. Nonetheless, almost 50% of the identified transcripts showed an increased level in the wildtype, when compared with the mutant. Recent studies demonstrated that RNases J1/J2 of *B. subtilis* can alter gene expression by modulating transcript stability [54]. In addition, the absence/decrease of RNases J1/J2 results in similar numbers of transcripts whose abundance is either increased or decreased, suggesting a complex role of these ribonucleases in both degradative and regulatory processing events [54]. Thus, the altered levels in the presence and absence of a given RNase of many transcripts may result from a perturbation of the expression levels of a limited number of genes and may thus result from indirect effects. In any case, almost one half of the detected transcripts displayed an increased level in MW001Δ2362. Using the COG database tool [56] we predicted the function of all 667 affected RNAs. However, no common feature or function among these transcripts could be identified. 45% are unknown and the function of approximately 55% are associated with inorganic ion transport, amino acid transport and metabolism, secretion and vesicular transport, energy production and cell motility. (Fig. 23).

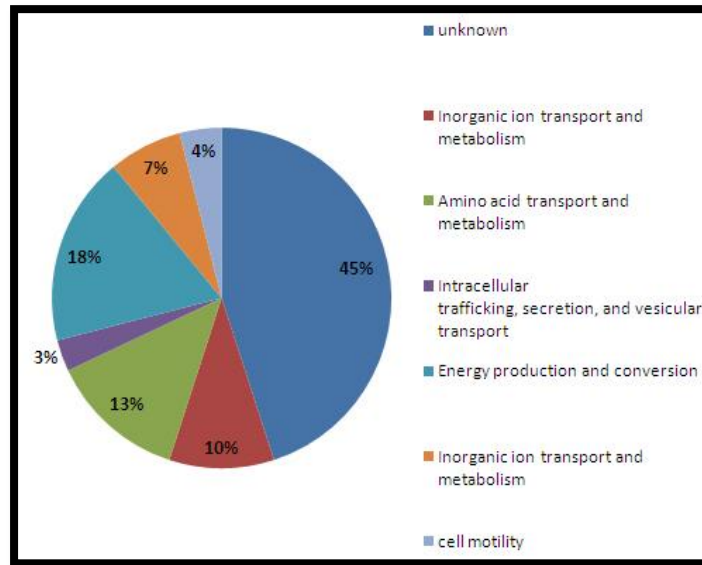


Figure 23. Functional classification of transcripts affected by RNase J. Each affected transcript was assigned to a certain class, using the COG database tool [56]. The fisher p-value for this functional prediction analysis was calculated with the fisher exact method and the significant level was set to 5%. 45% = unknown; 10% = inorganic ion transport and metabolism; 13% = amino acid transport and metabolism; 3% = intracellular trafficking, secretion and vesicular transport; 18% = energy production and conversion; 7% = inorganic ion transport and metabolism; 4% = cell motility.

As mentioned above, many of the affected RNAs may not be direct substrates of Sact-RNase J and it is therefore difficult to predict if Sact-RNase J affects particular pathways or functions in the cell.

In an attempt to reveal direct substrates of Sact-RNase J, we screened the data for transcripts, which (i) are more abundant in the *Saci_2362* deletion strain and (ii) for which a decreased read coverage of the 5'-end was observed. 14 transcripts, fulfilling these criteria, were detected in logarithmically growing cells, whereas 13 were found during stationary phase of growth. Three of these "logarithmic phase " transcripts encode ribosomal proteins (Tab. 3), which raises the question whether Sact-RNase J plays a role in the biogenesis and maturation of ribosomes. Given that *B. subtilis* RNase J1 is involved in 16S rRNA maturation, which is triggered by its 5'-to- 3' exoribunclease activity [12] another candidate is *Saci_1516*, encoding for 5S ribosomal RNA in *S. acidocaldarius*. Although the bioinformatic analyzes did not detect a 5'-to- 3' degradation for this transcript, we observed a significant upregulation (log2 fold change $\approx 1,5$) in the mutant, suggesting an impact of Sact-RNase J on this rRNA. It is known that RNase J1 and J2 form a complex in *B. subtilis*, that confers endonuclease activity [57]. Interestingly, the endonucleolytic cleavage specificity mediated by

the complex appears to vary from the individual enzymes *in vitro* [58]. As we were focusing on targets that are degraded from the 5'-end, and we cannot exclude endonucleolytic activity of SacI-RNase J on certain substrates, some targets may have escaped our bioinformatic analysis.

It was shown that the absence or decrease of both, RNase J1 and J2, profoundly alters the expression level of hundreds of genes in *B. subtilis* [54]. In contrast, the effect on global gene expression was minimal in single mutant strains, suggesting that two nucleases have largely overlapping substrates specificities [54]. As SacI-RNase J is not essential in *S. acidocaldarius*, we addressed the question whether other possible RNase J proteins exist in *S. acidocaldarius*. A homology search for *S. acidocaldarius* proteins comprising motif 2 was done, using blastp (<http://blast.ncbi.nlm.nih.gov>). We obtained a protein termed SacI-1807 and although the alignment with SacI-2362 shows a 12,2 % overall homology, motif 2 is conserved except for two substitutions (Valine → Isoleucine, Lysine → Glycine) (Fig. 24). From the RNAseq. data *Saci_1807*, like *Saci_2362*, is more abundant during logarithmic growth. Clearly this finding poses the question to the existence and function of other RNase J-like proteins in *S. acidocaldarius*. Similar to the RNases in *B. subtilis*, these enzymes could form a complex with SacI-RNase J and could jointly affect turnover of RNAs.

8. Appendix

8.1. Buffers and solutions

100x Brock's

$(\text{NH}_4)_2\text{SO}_4$	130 g/l
$\text{MgSO}_4 \times 7 \text{ H}_2\text{O}$	25 g/l
$\text{FeCl}_3 \times 6 \text{ H}_2\text{O}$	2 g/l

200x Brock's

KH_2PO_4	56 g/l
MnCl_2	360 mg/l
ZnSO_4	44 mg/l
CuCl_2	10 mg/l
VOSO_4	6 mg/l
Na_2MoO_4	6 mg/l
$\text{Na}_2\text{B}_4\text{O}_7$	0,9 mg/l

Autoclave, add 5ml 50% H_2SO_4

1000x Brock's

$\text{CaCl}_2 \times 2 \text{ H}_2\text{O}$	70 g/l ddH_2O
--	-------------------------------

Autoclave

DEPC-H₂O

1ml/l Diethylpyrocarbonat (DEPC) → o/n on RT → autoclave

RNA elution buffer

KOAc	0,6 M
EDTA	0,1 mM

Protein-Gels:

TBE (10x)

Tris	108 g/l
Boric acid	55 g/l
0,5M EDTA, pH 8	100 ml/l

30% PAA stock solution (29:1)

Acrylamide	290 g
N-N-methylenbisacrylamide	10 g
ddH_2O	add to 1L

40% PAA stock solution (29:1)

Acrylamide	380 g
N-N-methylenbisacrylamide	20 g
ddH ₂ O	add to 1L

SDS running buffer (x10)

Tris	30 g/l
Glycin	144 g/l

Add 5ml SDS (20%) for x1

SDS-Gel (Separating), 1 Gel

	8 % (μl)	10 % (μl)	12 % (μl)	15 % (μl)
H ₂ O	2,9	2,5	2,1	1,5
L-Tris	1,5	1,5	1,5	1,5
30%PAA	1,6	2	2,4	3

Add 14μl of APS (10%) and 7μl of TEMED for each gel

SDS-Gel (Collecting), 1Gel

	(ml)
H ₂ O	1,5
U-Tris	0,6
30%PAA	0,27

Add 10μl of APS (10%) and 10μl of TEMED for each gel

Loading buffer (x2)

Tris-HCl pH 6.8	100 mM
SDS	4 %
Glycerol	20 %
β-Mercaptoethanol	1 %

Destain solution

Methanol	45 %
Acetic Acid	10 %
In ddH ₂ O	

Coomassie staining solution

Methanol	45 %
Acetic Acid	10 %
Coomassie Blue	0,25 %
In ddH ₂ O	

Laemmli Buffer (1x)

Tris pH6.8	50 mM
SDS	2 %
Glycerol	10 %
Bromphenol Blue	0,1 %
β-Mercaptoethanol	1 %

DNA-Gel:

Gel for RNA assay

PAA	20 %
Urea	7 M
In 1xTBE	

Reaction buffer for RNAase assay

MgCl ₂	10 mM
KCl	10 mM
Tris-HCl pH 7.5	5 mM

Agarosegel (0,8%)

Agarose	2,4 g
TBE(x0,5)	Add to 300ml

DNA loading dye

Tris pH 7.6	10 mM
Orange G	0.15 %
Xylene Cyanol FF	0.03 %
Glycerol	60 %
EDTA	60 mM

Northern-blot:

Washing solutions

20x saline-sodium citrate (SSC) buffer (2l)	350,6 g NaCl	177,4g Na-citrat	Adjust pH to 7 with NaOH
Washing solution I (2l)	200 ml SSC (20x)	10 ml 20 % SDS	
Washing solution II (2l)	10 ml SSC (20x)	10 ml 20 % SDS	

Protein purification buffers:

Native conditions

Buffer	Imidazol	NaH ₂ PO ₄	NaCl
Lysis-buffer	10 mM	50 mM	300 mM
Wash-buffer	20 mM	50 mM	300 mM
Elution-buffer	250 mM	50 mM	300 mM

Denaturing conditions

Buffer	NaH ₂ PO ₄	Tris·Cl	Urea	pH
Lysis-buffer	100 mM	10 mM	8 M	8.0

Wash-buffer	100 mM	10 mM	8 M	6.3
Elution-buffer I	100 mM	10 mM	8 M	5.9
Elution-buffer II	100 mM	10 mM	8 M	4.5

General reaction mixes:

Reaction mix for DNA-oligonucleotide labeling

DNase free H ₂ O	13 µl
Primer (10pmol/µl)	2 µl
[γ- ³² P]ATP	2 µl
T4 PNK (Fermentas)	2 µl
10x PNK buffer A (Fermentas)	2 µl

Ambion MEGAscript T7 Kit T7

Buffer	2 µl
DTT	2 µl
Enzyme mix	2 µl
each C, U, G (10 mM)	1 µl
Alpha-ATP ³² (radioactive, 10mCi/ml)	2 µl
DEPC- _{dd} H ₂ O	3 µl

8.2. General protocols

Gelrite plates (1l) for *Sulfolobus solfataricus*

6.4 g of gelrite (gellan gum, Kelco Biopolymers) were boiled in 500 ml of _{dd}H₂O. In parallel 500 ml of double concentrated Brock's medium were prepared and 6 ml of 0.5 M CaCl₂ and 10 ml of 1 M MgCl₂ were added and pre-warmed to 60°C. The medium was slowly poured in the gelrite solution and pH was adjusted to 3.5 using sulfuric acid [47].

Glycerol stocks of *S. solfataricus* and *S. acidocaldarius*

10 ml of logarithmically growing *Sulfolobus* cells (OD₆₀₀ of 0,4) were pelleted (4°C / 4000 rpm) and resuspended in Brock's salts solution containing 25% glycerol. Stocks were stored at -80°C.

Competent *E. coli* cells

50 ml of logarithmically growing *E. coli* cells (OD₆₀₀ of 0,5) were pelleted (4°C / 4000 rpm) and washed with 0,1 M CaCl₂ (ice). Cells were constantly kept on ice

and finally resuspended in 2 ml CaCl_2 and 10% glycerol was added. Competent cells were stored at -80°C .

Transformation of competent *E. coli* cells

The ligation mix (T4-DNA ligase, Fermentas) was incubated for 10 min at 65°C to inactivate ligase. Subsequently, the competent cells were added and incubated for 5 min on ice. The samples were incubated for 3' at 42°C and cooled on ice for 3 min. 700 μl liquid LB-medium was added and the cells were incubated for 1h at 37°C on a thermocycler. Afterwards, the cells were spread on solid LB-medium containing the required antibiotics for plasmid selection.

Phenol / CHCl_3 DNA purification

50 μl Phenol and 50 μl CHCl_3 were added to 100 μl DNA mix. The sample was centrifuged (15000 rpm / RT / 3 min) and supernatant was carefully transferred into a new tube. 100 μl CHCl_3 was added, vortexed and again centrifuged (15000 rpm / RT / 3'). The supernatant was transferred to a new tube and 2,5 volume of 96 % EtOH and 1/10 volume of 3 M NaOAc was added. The mixture was incubated for 1h at -20°C and then centrifuged (13,000 rpm / 4°C / 15 min). The pellet was washed with 70% EtOH, dried and resuspended in ddH_2O .

Total RNA preparation with Trizol

A pellet from a 10 ml culture (OD_{600} of 0,4) was resuspended in 1.0 ml Trizol (TRIzol®, Invitrogen) and incubated at 65°C for 10 min, until it became translucent. 200 μl CHCl_3 was added and then the sample was vortexed. The sample was incubated at room temperature for 5 min. The sample was centrifuged at 15,000 rpm for 15 min at RT. The aqueous layer was transferred into a new tube and 500 μl of isopropanol was added. To precipitate RNA, the sample was kept for 1h at -20°C . After incubation at -20°C the RNA was centrifuged at 15,000 rpm for 30' and the pellet was washed with 70% ethanol (1.0 ml). After another centrifugation step at 15,000 rpm for 5 min at RT, EtOH was removed and the pellet was dried at room temperature. Finally, the RNA was resuspended in DEPC treated ddH_2O .

Total protein extracts from *S. acidocaldarius*

200 ml of *S. acidocaldarius* cells were grown to an OD₆₀₀ of 0,4 and 0,9, respectively. The cells were pelleted and resuspended in buffer A (20 mM Tris/HCl pH 7.4; 10 mM MgAcetat; 50 mM NH₄Cl; 1 mM DTT). Afterwards lysozyme (Biomol) was added and the samples were incubated for 30 min at 4°C. The cells were broken by sonication and centrifuged at 30.000 g, 30 min at 4°C. The protein extracts were aliquoted and stored at -80°C.

References

1. Egorova, K. and G. Antranikian, (2005) *Industrial relevance of thermophilic Archaea*. Curr Opin Microbiol, **8**(6): 649-655.
2. Belasco, J.G., (2010) *All things must pass: contrasts and commonalities in eukaryotic and bacterial mRNA decay*. Nat Rev Mol Cell Biol, **11**(7): 467-478.
3. Condon, C., (2003) *RNA processing and degradation in Bacillus subtilis*. Microbiol Mol Biol Rev, **67**(2): 157-174.
4. Apirion, (1973) *D. Degradation of RNA in Escherichia coli. A hypothesis*. Mol Gen Genet, **122**: 313–322.
5. Celesnik, H., A. Deana, and J.G. Belasco, (2007) *Initiation of RNA decay in Escherichia coli by 5' pyrophosphate removal*. Mol Cell, **27**(1): 79-90.
6. Deutscher, M.P., (2006) *Degradation of RNA in bacteria: comparison of mRNA and stable RNA*. Nucleic Acids Res, **34**(2): 659-666.
7. Callaghan, A.J., et al., (2005) *Structure of Escherichia coli RNase E catalytic domain and implications for RNA turnover*. Nature, **437**(7062): 1187-1191.
8. Carpousis, (2007) *The RNA degradosome of Escheria coli: an mRNA-degrading machine assembled on RNase E*. Annu Rev Microbiol, **61**: 71-87.
9. McDowall, K.J., S. Lin-Chao, and S.N. Cohen, (1994) *A+U content rather than a particular nucleotide order determines the specificity of RNase E cleavage*. J Biol Chem, **269**(14): 10790-10796.
10. Sandler, P. and B. Weisblum, (1988) *Erythromycin-induced stabilization of ermA messenger RNA in Staphylococcus aureus and Bacillus subtilis*. J Mol Biol, **203**(4): 905-915.
11. Even, S., et al., (2005) *Ribonucleases J1 and J2: two novel endoribonucleases in B.subtilis with functional homology to E.coli RNase E*. Nucleic Acids Res, **33**(7): 2141-2152.
12. Mathy, N., et al., (2007) *5'-to-3' exoribonuclease activity in bacteria: role of RNase J1 in rRNA maturation and 5' stability of mRNA*. Cell, **129**(4): 681-692.
13. Li de la Sierra-Gallay, I., et al., (2008) *Structural insights into the dual activity of RNase J*. Nat Struct Mol Biol, **15**(2): 206-212.
14. Callebaut, I., et al., (2002) *Metallo-beta-lactamase fold within nucleic acids processing enzymes: the beta-CASP family*. Nucleic Acids Res, **30**(16): 3592-3601.

15. Commichau, F.M., et al., (2009) *Novel activities of glycolytic enzymes in Bacillus subtilis: interactions with essential proteins involved in mRNA processing*. Mol Cell Proteomics, **8**(6): 1350-1360.
16. Shahbadian, K., et al., (2009) *RNase Y, a novel endoribonuclease, initiates riboswitch turnover in Bacillus subtilis*. EMBO J, **28**(22): 3523-3533.
17. Yao, S. and D.H. Bechhofer, (2010) *Initiation of decay of Bacillus subtilis rpsO mRNA by endoribonuclease RNase Y*. J Bacteriol, **192**(13): 3279-3286.
18. Tourriere, H., K. Chebli, and J. Tazi, (2002) *mRNA degradation machines in eukaryotic cells*. Biochimie, **84**(8): 821-837.
19. Tharun, S., et al., (2000) *Yeast Sm-like proteins function in mRNA decapping and decay*. Nature, **404**(6777): 515-518.
20. Achsel, T., et al., (1999) *A doughnut-shaped heteromer of human Sm-like proteins binds to the 3'-end of U6 snRNA, thereby facilitating U4/U6 duplex formation in vitro*. EMBO J, **18**(20): 5789-5802.
21. Collins, B.M., et al., (2001) *Crystal structure of a heptameric Sm-like protein complex from archaea: implications for the structure and evolution of snRNPs*. J Mol Biol, **309**(4): 915-923.
22. Hasenöhrl, D., R. Konrat, and U. Bläsi, (2011) *Identification of an RNase J ortholog in Sulfolobus solfataricus: implications for 5'-to-3' directional decay and 5'-end protection of mRNA in Crenarchaeota*. RNA, **17**(1): 99-107.
23. Evguenieva-Hackenberg, E., et al., (2003) *An exosome-like complex in Sulfolobus solfataricus*. EMBO Rep, **4**(9): 889-893.
24. Franzetti, B., et al., (1997) *Biochemical and serological evidence for an RNase E-like activity in halophilic Archaea*. J Bacteriol, **179**(4): 1180-1185.
25. Allmang, C., et al., (1999) *The yeast exosome and human PM-Scl are related complexes of 3' --> 5' exonucleases*. Genes Dev, **13**(16): 2148-2158.
26. Mitchell, P., et al., (1997) *The exosome: a conserved eukaryotic RNA processing complex containing multiple 3'-->5' exoribonucleases*. Cell, **91**(4): 457-466.
27. Buttner, K., K. Wenig, and K.P. Hopfner, (2005) *Structural framework for the mechanism of archaeal exosomes in RNA processing*. Mol Cell, **20**(3): 461-471.

28. Hasenöhrl, D., *et al.*, (2008) *Translation initiation factor a/elf2(-gamma) counteracts 5' to 3' mRNA decay in the archaeon Sulfolobus solfataricus*. Proc Natl Acad Sci U S A, **105**(6): 2146-2150.
29. Ludwig, W., *et al.*, (2004) *ARB: a software environment for sequence data*. Nucleic Acids Res, **32**(4): 1363-1371.
30. De la Sierr-Gallay IL, Z., Jamalli A, Putzer H., (2008) *Structural insights into the dual*. Nat Struct Mol Biol, **15**(2): 206-212.
31. Konrat, R., (2009) *The protein meta-structure: a novel concept for chemical and molecular biology*. Cell Mol Life Sci, **66**(22): 3625-3639.
32. Clouet-d'Orval, B., *et al.*, (2010) *Euryarchaeal beta-CASP proteins with homology to bacterial RNase J Have 5'- to 3'-exoribonuclease activity*. J Biol Chem, **285**(23): 17574-17583.
33. Pedulla, N., *et al.*, (2005) *The archaeal elf2 homologue: functional properties of an ancient translation initiation factor*. Nucleic Acids Res, **33**(6): 1804-1812.
34. Schmitt, E., S. Blanquet, and Y. Mechulam, (2002) *The large subunit of initiation factor aIF2 is a close structural homologue of elongation factors*. EMBO J, **21**(7): 1821-1832.
35. Yatime, L., *et al.*, (2004) *Functional molecular mapping of archaeal translation initiation factor 2*. J Biol Chem, **279**(16): 15984-15993.
36. Nikonov, O., *et al.*, (2007) *New insights into the interactions of the translation initiation factor 2 from archaea with guanine nucleotides and initiator tRNA*. J Mol Biol, **373**(2): 328-336.
37. Nercessian, D. and R.D. Conde, (2006) *Control of ribosome turnover during growth of the haloalkaliphilic archaeon Natronococcus occultus*. Res Microbiol, **157**(7): 625-628.
38. Cellini, A., *et al.*, (2004) *Stringent control in the archaeal genus Sulfolobus*. Res Microbiol, **155**(2): 98-104.
39. Miller, J.H., (1972) *Experiments in Molecular Genetics*. Cold Spring Harbor Laboratory, Cold Spring Harbor, NY1972.
40. Brock, T.D., *et al.*, (1972) *Sulfolobus: a new genus of sulfur-oxidizing bacteria living at low pH and high temperature*. Arch Mikrobiol, **84**(1): 54-68.
41. Wagner, M., *et al.*, (2009) *Expanding and understanding the genetic toolbox of the hyperthermophilic genus Sulfolobus*. Biochem Soc Trans, **37**(Pt 1): 97-101.

42. Londei, P., et al., (1986) *Differential features of ribosomes and of poly(U)-programmed cell-free systems derived from sulphur-dependent archaeobacterial species*. Eur J Biochem, **157**(3): 455-462.
43. Steffan N. Hoa, H.D.H., Robert M. Hortonb, Jeffrey K. Pullena, Larry R., (1989) *Site-directed mutagenesis by overlap extension using the polymerase chain reaction*. Gene, **77**(1): 51-59.
44. Berkner, S., et al., (2007) *Small multicopy, non-integrative shuttle vectors based on the plasmid pRN1 for Sulfolobus acidocaldarius and Sulfolobus solfataricus, model organisms of the (cren-)archaea*. Nucleic Acids Res, **35**(12): e88.
45. Mortazavi, A., et al., (2008) *Mapping and quantifying mammalian transcriptomes by RNA-Seq*. Nat Methods, **5**(7): 621-628.
46. Hottes, A.K., et al., (2004) *Transcriptional profiling of Caulobacter crescentus during growth on complex and minimal media*. J Bacteriol, **186**(5): 1448-1461.
47. Albers, D., (2007) *Conditions for genedisruption by homologous recombination of exogenous DNA into the Sulfolobus solfataricus genome*. Archaea2, 145-149 published online.
48. Washietl S., et.al., (2005) *Fast and reliable prediction of noncoding RNAs*. Proc. Natl. Acad. Sci. U S A, **102**: 2454-2459.
49. E. P. Nawrocki, et.al., (2009) *Infernal 1.0: Inference of RNA alignments* . Bioinformatics, **25**: 1335-1337.
50. Simon Anders et. al., (2010) *Differential expression analysis for sequence count data*. Genome Biology, **11**: R106 (open access).
51. Deana, A., H. Celesnik, and J.G. Belasco, (2008) *The bacterial enzyme RppH triggers messenger RNA degradation by 5' pyrophosphate removal*. Nature, **451**(7176): 355-358.
52. Newbury, S.F., (2006) *Control of mRNA stability in eukaryotes*. Biochem Soc Trans, **34**(Pt 1): 30-34.
53. She, Q., et al., (2001) *The complete genome of the crenarchaeon Sulfolobus solfataricus P2*. Proc Natl Acad Sci U S A, **98**(14): 7835-7840.
54. Mäder U. et al., (2008) *mRNA processing by RNase J1 and J2 affects Bacillus subtilis gene expression on a global scale*. Molecular Microbiology, **70**(1): 183-196.
55. Mathy N, et al., (2010) *Bacillus subtilis ribonucleases J1 and J2 form a complex with altered enzyme behaviour*. Molecular Microbiology, **75**: 489-498.

56. Roman L., Tatusov *et al.*, (2000) *The COG database: a tool for genome-scale analysis of protein functions and evolution*. Nucleic Acids Res, **28**(1): 33–36.
57. Condon Ciarán, (2010) *What is the role of RNase J in mRNA turnover?* RNA Biology, **7**(3): 316-321.
58. Mathy N. *et al.*, (2010) *Bacillus subtilis ribonuclease J1 and J2 form a complex with altered enzyme behavior*. Molecular Microbiology, **75**: 489-498.
59. Hoffmann S. *et. al.*, (2009) *Fast mapping of short sequences with mismatches, insertions and deletions using index structures*. PLoS Comput Biol, **5**(9): e1000502

Appendix II

Sso-2509

In *E.coli* and in *Eukaryotes*, enzymes have been identified that remove the protective tri-phosphate or the cap structure, which in both cases result in a mono-phosphorylated 5'-terminus [1, 2]. The mono-phosphorylated 5'-ends are considered to be suitable substrates for 5'-to- 3' exonucleases. In *Sulfolobus solfataricus* the translational initiation factor a/eIF2 (γ) counteracts 5'-to- 3' directional decay of mRNA [3]. However, it is unknown how a/eIF2 is recycled from the 5'-ends of transcripts. The *S. solfataricus* protein 2509 has been shown to interact with the γ -subunit of Sso-a/eIF2 (B. Märtens, unpublished results). This raises the question whether Sso-2509 can remove the factor from the tri-phosphate 5'-terminus of mRNAs. Sso-2509 was identified by bio-affinity chromatography using *S. solfataricus* lysate and purified a/eIF2 (γ)-His-tag attached to a Ni-NTA column. A subsequent mass spectrometry analysis revealed a co-elution of Sso-2509 with a/eIF2 (γ) (B. Märtens, unpublished results). It was further shown that only protein extracts derived from cultures, after outgrowth from stationary phase, contained Sso-2509. The 14,788 kDa protein contains a predicted Zn-ribbon, a typically structural motif for nucleic acid binding proteins. In addition, BLAST search revealed that Sso-2509 comprises a DUF35 domain (conserved domain of unknown function).

Here, we addressed the question during which growth phase *Sso_2509* is expressed and to which extent a deletion of 2509 influences growth and in particular outgrowth of cells from stationary phase.

Table 1. Strains, plasmid and primers used in this study

Strains	Description	Source
<i>Sulfolobus solfataricus</i> M16	<i>pyER⁻, lacS⁻</i>	[3]
Sso-M16 2508/09-lacS	Containing construct 2508/09- <i>lacS</i>	This study
Sso-PBL2025Δ2509	<i>pyER⁺, lacS⁺, Δ2509</i> (gene, encoding for Sso-2509 is deleted)	This study
<i>E.coli</i>-TOP 10	F- <i>mcrAΔ (mrrhsdRMSm crBC) ϕ80lacX74 nupG recA1 araD139 Δ(ara-leu) 7697galE15galK16rpsL (Str^R)</i>	Invitrogen
<i>E.coli</i>-BL21 (Rosetta)	F ⁻ , <i>dcm, ompT, hsdS(rB-mB-), galλ(DE3)</i>	Stratagene
Sso-PBL2025	<i>pyER⁺, lacS⁻</i>	[4]

Plasmids	Description	Source
pET2268	<i>lacS</i> cassette with its own promoter and terminator region	[5]
pET2268-Δ2509	Plasmid with Sso_2509 flanking region	This study
pSVA5	cloning vector, contains the ara-promotor and <i>lacS</i> , (Amp ^R)	[6]
pSVA5-2508/09-lacS	2508/09 cloned in pSVA5 and fused to <i>lacS</i>	This study (5.2.2.)
pMJ05	<i>E.coli</i> - Sso shuttle vector, contains <i>pyER</i> from <i>S. solfataricus</i>	[6, 7]
pMJ05-2508/09-lacS	2508/09- <i>lacS</i> construct cloned in pMJ05	This study (5.2.2.)

Oligo-nucleotides	Sequence	Description	Genome-coordinates
S71_2509KO_Up_FP	5'-TCT <u>GGTACCGAACAAGGT</u> TTTTTAATAGGTAGTA -3'	SSo-2509 up-stream region forward primer, cleavage site for <i>KpnI</i> (underlined)	Start: 2276600 End: 2277772
T71_2509KO_Up_RP	5'-TCT <u>CCATGGCGCTCACC</u> CAATACTAAAGTTAC AC-3'	SSo_2509 up-stream region reverse primer, cleavage site for <i>NcoI</i> (underlined)	Start: 2276600 End: 2277772
U71_2509KO_down_FP	5'-TCT <u>GGATCCCTTTTAATC</u> ATTCACAATATGATC -3'	SSo_2509 down-stream region reverse primer, cleavage site for <i>BamHI</i> (underlined)	Start: 2278146 End: 2280225
V71_2509KO_down_RP	5'-TCT <u>GCGGCCGCACCTTTA</u>	SSo_2509 down-stream region re-	Start: 2278146

	TTCTGTACTCTTCTAA T-3',	verse primer, cleavage site for <i>NotI</i> (underlined)	End: 2280225
2509_KOtest _FP	5'-AGGTAGT TTAAATACTGGTCAG CCC-3'	Verification of dele- tion of Sso-2509, forward primer	Start: 2277588 End: 2277612
2509KO_test _RP	5'- ATAGCCCGTCATCAG TATGGAGTTC-3'	Verification of dele- tion of Sso-2509, reverse primer	Start: 2278223 End: 2278247
2508/9_FP	5'-TTTCCTAGGTG TAATGGGGAGACTCA GGTTTCCT-3'	2508/09 and 2508/09- <i>lacS</i> for- ward primer, cleavage site for <i>XmaI</i> (underlined)	Start: 2276377 End: 2276401
2508/9_RP	5'-TTTCCATGGCTAA CTTATTCTCATCGA AATACTT-3	2508/09 reverse primer, cleavage site for <i>NcoI</i> (un- derlined)	Start: 2277804 End: 2277827
pMJ05lacS_ RP	5'-CCCAGCGCGT CGGCCGGCAATCTA ATGAAAAT-3'	2508/09- <i>lacS</i> re- verse primer, cleavage site for <i>EagI</i> (underlined)	Start: 2768163 End: 2768178

1. Materials and Methods

1.1. Construction of plasmids

psVA5-2508/09-*lacS* and pMJ05-2508/09-*lacS*

The region, 1395 bp upstream of *Sso_2509* and 57 bp downstream of the start-codon (ATG) of *Sso_2509* was amplified by PCR from genomic DNA isolated from *S. solfataricus* M16, using primers 2508/09_FP: 5'-TTTCCTAGG TGTAATGGGGAGACTCAGGTTTCCT-3' and 2508/09_RP: 5'-CCCAGCG CGTCGGCCGGCAATCTAATGAAAAT-3' (Table 1). The resulting PCR product termed 2508/09 contained the promoter region of *Sso_2509* and in addition the first nineteen codons of *Sso_2509*. *NcoI* and *XmaI* cleavage sites were introduced to insert the fragment into vector psVA5, thereby creating an in frame *lacS*-fusion (Fig. 1). The obtained plasmid pSVA5-2508/09-*lacS* (Fig. 1) was used as template for PCR amplification of the construct termed 2508/09-*lacS* (Fig. 2). To amplify 2508/09-*lacS*, the primers 2508/09_FP and pMJ05*lacS*_RP: 5'-CCCAGCGCGTCGGCCGG CAATCTAATGAAAAT-3' were used. The PCR product (2508/09-*lacS*) was digested with *XmaI* and *EagI* and ligated into pMJ05. The plasmid pMJ05 is a shuttle vector, containing the *pyrER* locus, that complements the uracil auxotroph mutant strain *Sulfolobus solfataricus* M16. The recombinant plasmid pMJ05-2508/09-*lacS* was transformed into *E.coli* Top 10 cells (Invitrogen). Afterwards the plasmid was purified from Top 10 cells and used as a PCR template, using the primers 2508/09_FP and pMJ05*lacS*_RP. The analysis yielded the fragment with the expected size, indicating that pMJ05 contained the 2508/09-*lacS* construct. The vector pMJ05-2508/09-*lacS* was transformed in *S. solfataricus* M16 by electroporation [5] (see 1.2.). Transformants containing the recombinant plasmid pMJ05-2508/09-*lacS* grew in uracil minimal media. To obtain simple 2508/09-*lacS* containing cells, they were spread on gelrite plates (without uracil) and sprayed with 2% X-gal in Dimethylformamid (DMF). Blue colonies were inoculated in Brock's medium without uracil and used for further experiments.

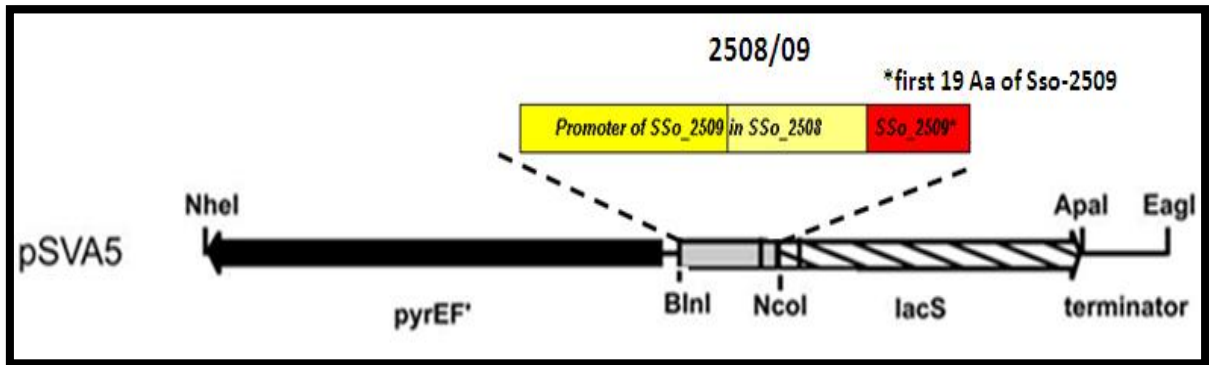


Figure 1. The construct 2508/09 was cloned into the Vector pSVA5 and thereby fused with *lacS*. *BlnI* = *XmaI*. The obtained recombinant vector is termed pSVA5-2508/09-*lacS*

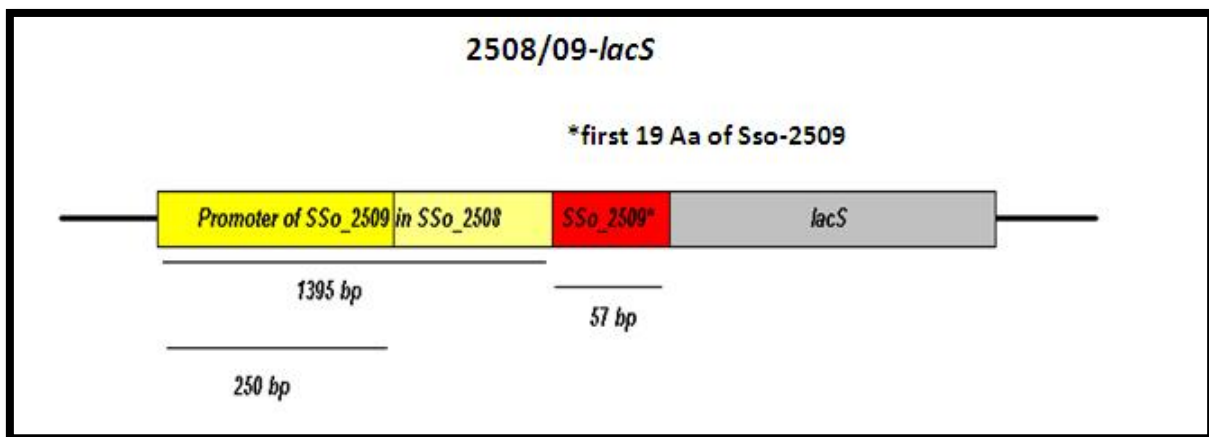


Figure 2. Construct 2508/09-*lacS*. It contains the 1395 bp upstream flanking region of *Sso_2509* (including the promoter region of *Sso_2509*), the 57 base pairs (encoding for the first nineteen amino acids of *Sso-2509*) and *lacS*.

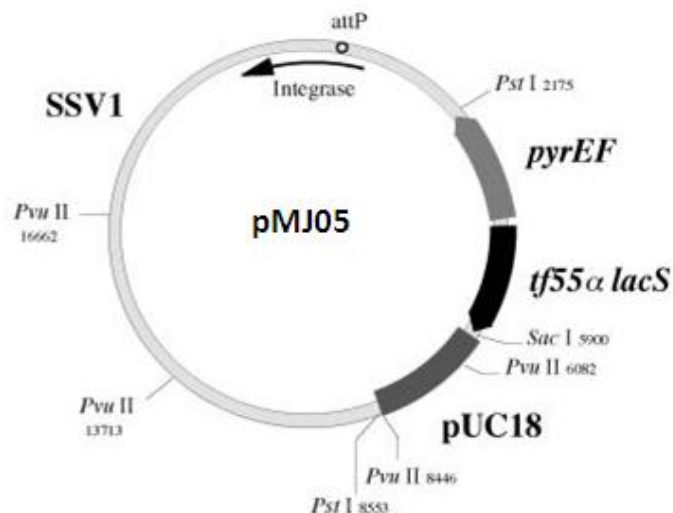


Figure 3. The shuttle vector pMJ05 based on the virus SSV1. The vector harbors the *pyrEF* cluster, complementing uracil auxotrophy.

1.2. Electroporation of *Sulfolobus solfataricus*

Transformation of *Solfataricus* cells was performed as described by Schleper *et al.* [8]. A culture of *Sulfolobus solfataricus* M16 (*pyrEF/lacS* double mutant) was grown in 50 ml of Brock's medium (5.1.) until the cells reached an OD₆₀₀ between 0.2-0.3. The culture was cooled on ice and the cells were centrifuged for 20 min at 4000 rpm, 4°C. To decrease the amount of residual salt the cell pellet was washed three times with 20 ml of 20 mM sucrose (ice cold). Finally, the cells were resuspended in 20 mM sucrose and the cell number was adjusted to 10¹⁰ cells/ml. The cells were incubated on ice before electroporation, and aliquots (50 µl) were mixed with 300 ng DNA and transferred to electroporation cuvettes (Bio-rad). The high-voltage electroporation was performed with a Gene Pulser apparatus (Bio-Rad) (1.5 kV, 25 µF, 400 Ω). After electroporation 1 ml of medium was directly added and the cells were regenerated in a thermo-mixer at 75°C for 1h. Afterwards, the cells were inoculated into pre-warmed 50 ml cultures with Brock's medium containing uracil. The cultures were grown at 75°C until they reached an OD₆₀₀ of 0.5 (2-3 days), and subsequently transferred to selective medium without uracil. In case of *lacS* containing constructs a fast activity test was conducted. 800 µl of cell culture (OD₆₀₀ = 0.3-0.5) were mixed with 100 µl X-Gal (5 mg X-Gal per ml in dimethylformamid). The mixture was incubated at 75°C for 15-30 minutes until blue color appeared

1.3. β-galactosidase assay

The substrate *o*-Nitrophenyl-β-D-galactopyranoside (ONPG) was used for determining β-galactosidase activity. The ONPG hydrolysis reaction was followed spectrophotometrically at 70°C by measuring the increase in absorbance at 420 nm. A control containing all reactants except the enzyme was used to correct for thermal hydrolysis. *S. solfataricus* M16 harboring the plasmid pMJ05-2508/09-*lacS* (Tab. 1), was grown in Brock's medium at 75°C to an OD₆₀₀ of 1. Then, the cultures were diluted to an OD₆₀₀ of 0,25. 2 ml samples were taken before dilution and 0, 1h, 3h, 5h, 7h and 24h after dilution. At each time the OD₆₀₀ was determined. The cells were harvested by centrifugation (10000 rpm, 5 min), and the pellets were resuspended in 50 µl of ddH₂O. Samples were frozen with liquid nitrogen and thawed by incubation at 37°C. The lysate was mixed

with 950 µl of buffer, containing 50 mM sodiumphosphate pH=6.5, 4 mg/ml ONPG and incubated for 45 min at 70°C. To remove cell debris, the samples were centrifuged for 2 minutes at 13.000 rpm after incubation. The results were expressed in Miller-units as described in [9], using the equation

$$\frac{1000 * OD_{420} * (dilution) / t(min) * V(ml) * Od_{600}}{}$$

1.4. Construction of the (SSo-PBL2025 Δ 2509) deletion mutant

Construction of the deletion plasmid- Δ 2509

The deletion plasmid was constructed as described in [5]. The up- (1172 bp) and downstream (2079 bp) regions of *Sso_2509* were amplified by PCR from genomic DNA isolated from *S. solfataricus* PBL2025. The upstream flanking region was amplified with primers S71_2509KO_Up_FP: 5'-TCTGGTACCGAACAAGGTTTTTTAATAGGTAGTA-3' and T71_2509KO_Up_RP: 5'-TCTCCATGGCGCTCACCCAATACTAAAGTTACAC-3'. The PCR product (upstream region) was digested with *KpnI* and *NcoI* and ligated into pET2268, which contains the *lacS* cassette with its own promoter and terminator region (Fig. 4). The downstream flanking region was amplified with primers U71_2509KO_down_FP: 5'-TCTGGATCCCTTTTAATCATTTTACAATATGATC-3' and V71_2509KO_down_RP: 5'-TCTGCGGCCGCACCTTTATTCTGTACTCTTCTAAT-3'. The resulting product (downstream region) was digested with *BamHI* and *NotI* and ligated into pET2268 containing the upstream flanking region yielding pET2268- Δ 2509.

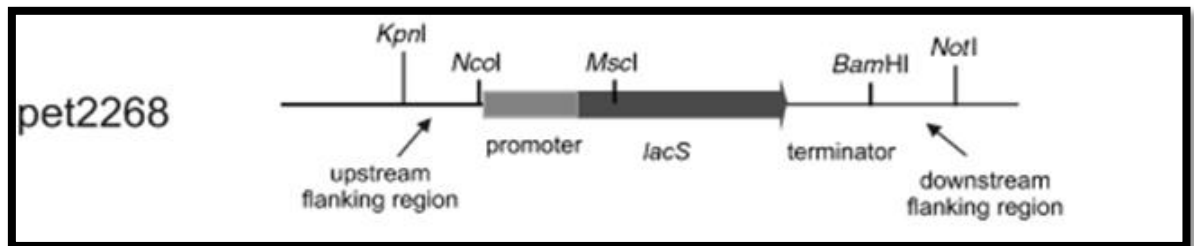


Figure 4. Schematic overview of plasmid pET2268 used for construction of the SSo_2509 deletion mutant in Sso-PBL2025. The *KpnI/NcoI* and *BamHI/NotI* restriction sites were used to insert the upstream and downstream flanking regions of SSo_2509 [5].

Construction of PBL2025 Δ 2509

The plasmid was transformed into PBL2025 as described in 1.2. After electroporation, the cells were resuspended in 1 ml of demineralized water, incubated briefly (1-3 min) on ice and then incubated 10 min at 75°C. The cells were transferred to 50 ml of pre-warmed lactose minimal medium (Brock's medium, supplemented with 0.4% lactose), (Tab. 1). After the culture reached an OD₆₀₀ of 0.1 (10-12 days) 3 ml were transferred to 50 ml of fresh lactose minimal medium. After 10 to 14 days the cells reached an OD₆₀₀ of about 0.4. The cells were spread on gelrite plates. After 7 days of growth at 75°C the colonies were sprayed with 2% X-gal in Dimethylformamid (DMF). Blue colonies were inoculated in Brock's medium supplemented with N-Z amine. Genomic DNA, of the cells growing on N-Z amine was isolated and subjected to PCR analysis. The PCR analysis with primers 2509_KOtest_FP : 5'-AGGTAGTTTAA ATACTGGT CAGCCC-3' and 2509KO_test_R P: 5'-ATAGCCCGTCATCAGTATGGAGT TC-3' yielded fragments of expected size (2242 bp) indicating that recombination had occurred at the correct site. In addition the PCR analysis yielded a second product (635 bp), indicating that the target gene was still present in the analyzed strain. To select the deletion strain, the cells were again plated on N-Z amine gelrite plates and single blue colonies were selected, and this was repeated until the PCR analysis no longer indicated the presence of the wildtype allele (2-3 rounds), (Fig. 6).

Results

Sso-2509 is believed to interact with α /eIF2 and could thereby release the factor from the mRNA. First, we addressed the question in which phases of growth the gene *Sso_2509* is expressed. In order to determine the expression level of *Sso_2509*, the construct 2508/09-*lacS* was designed, which contains the promoter of *Sso_2509*, the Shine-Dalgarno sequence and the first 19 codons of *Sso_2509*, fused to the *lacS* gene (Fig. 2A). *S. solfataricus* M16 cells, harboring 2508/09-*lacS* were grown in Brock's medium to stationary phase ($OD_{600} \approx 1$). After 6-fold dilution the cells were inoculated in fresh medium and incubated until the culture reached again stationary phase. Samples were taken at an OD_{600} of 1 before dilution and 0h, 1h, 3h, 5h, 7h and 24h after re-inoculation. Then the LacS activity was determined as described in 1.3. It was shown that only protein extracts derived from cultures, after outgrowth from stationary phase, contained Sso-2509 (B. Märten, unpublished results). Thus we expected that LacS activity would be upregulated during outgrowth. However, we did not observe an upregulation and moreover detected a constant level of β -galactosidase activity in stationary phase and during outgrowth (Fig. 5).

We next tested whether a deletion of *Sso_2509* affects growth in logarithmic phase, stationary phase and during outgrowth after dilution of a stationary phase culture. The construction of the *Sso_2509* deletion strain PBL2025 Δ 2509 is described in 1.4 (Fig. 6). *S. solfataricus* PBL2025 and PBL2025 Δ 2509 (Tab 1), were inoculated in either 50 ml Allen's medium [9] (supplemented with Wollins vitamins [10] and 0,2% sucrose) or in Brock's medium (supplemented with 0,2 % N-Z amine and 0,2% sucrose) and the OD_{600} was adjusted to 0,01-0,03. The cells were incubated at 75°C until they reached stationary phase (9 days, $OD_{600} \approx 1,7$). Then, the PBL2025 and PBL2025 Δ 2509 cultures were diluted with fresh medium to an OD_{600} of 0,25 and incubated for 48h. After 0h, 1h, 3h, 5h, 7h, 24h and 48h the OD_{600} was measured. When compared to wildtype, no differences in growth, neither during outgrowth nor in stationary phase were detected for the Sso-2509 deletion strain, (Fig. 7, 8).

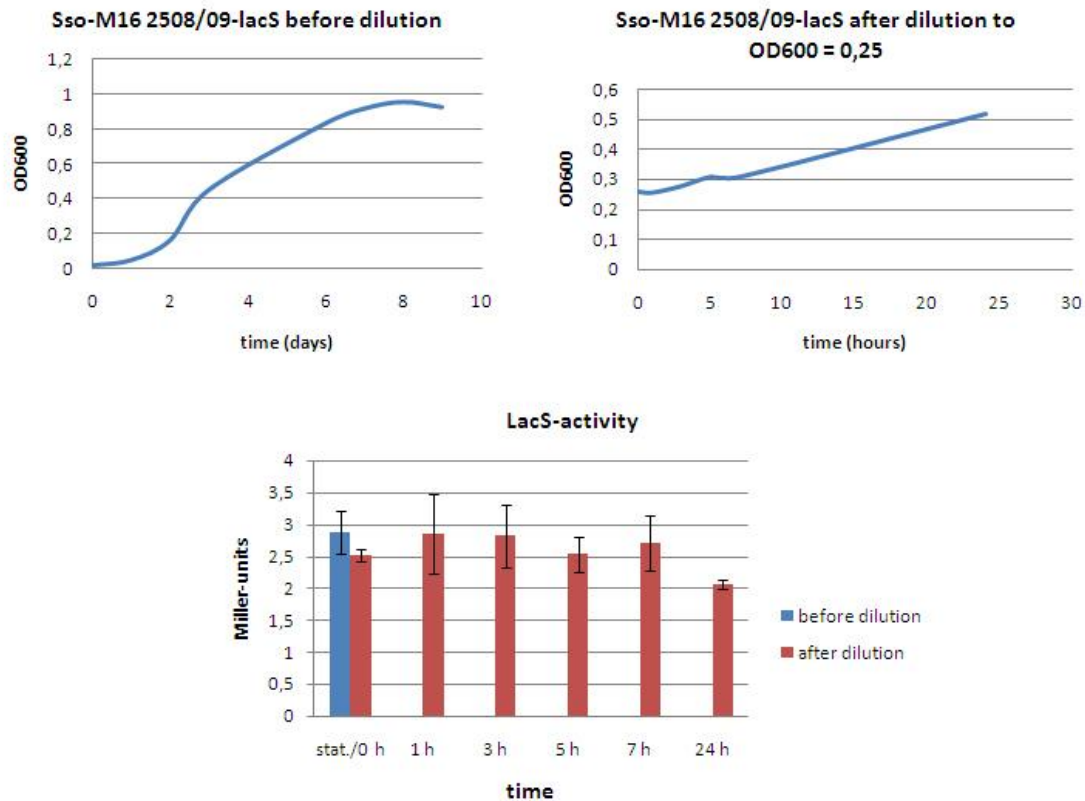


Figure 5. *S. solfataricus* M16 strain, harboring pMJ05-2508/09-*lacS*, was grown in Brock's medium to stationary phase ($OD_{600} \approx 1$) and then diluted in same medium to an OD_{600} of 0,25. Aliquots were taken before dilution and 0, 1h, 3h, 5h, 7h and 24h after dilution and the LacS activity was determined (3.4.). The upper panels show the growth of the corresponding culture before and after dilution, whereas the lower panel shows the β -galactosidase-assays [7]. The values are an average of three independent experiments.

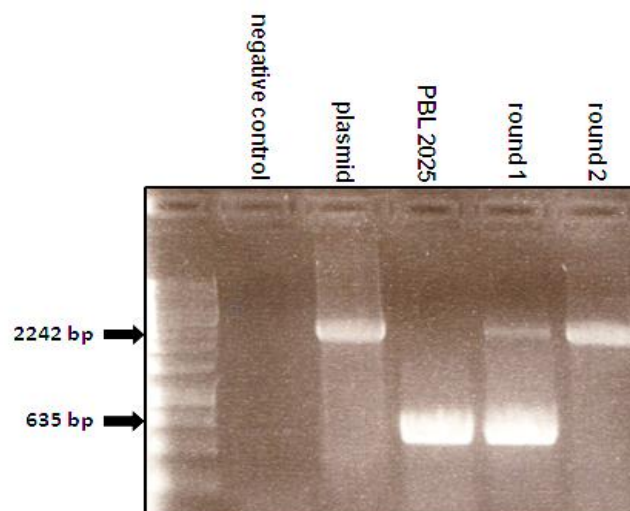


Figure. 6. Confirming the deletion of *Sso_2509* in strain *Sso*-PBL2025. Single colony picking was repeated, until PCR analysis no longer indicated the presence of the wildtype allele (635 bp). negative control = without template DNA; plasmid = pET2268- Δ 2509; PBL2025 = wildtype genomic DNA; round 1/2 = rounds of single colony picking.

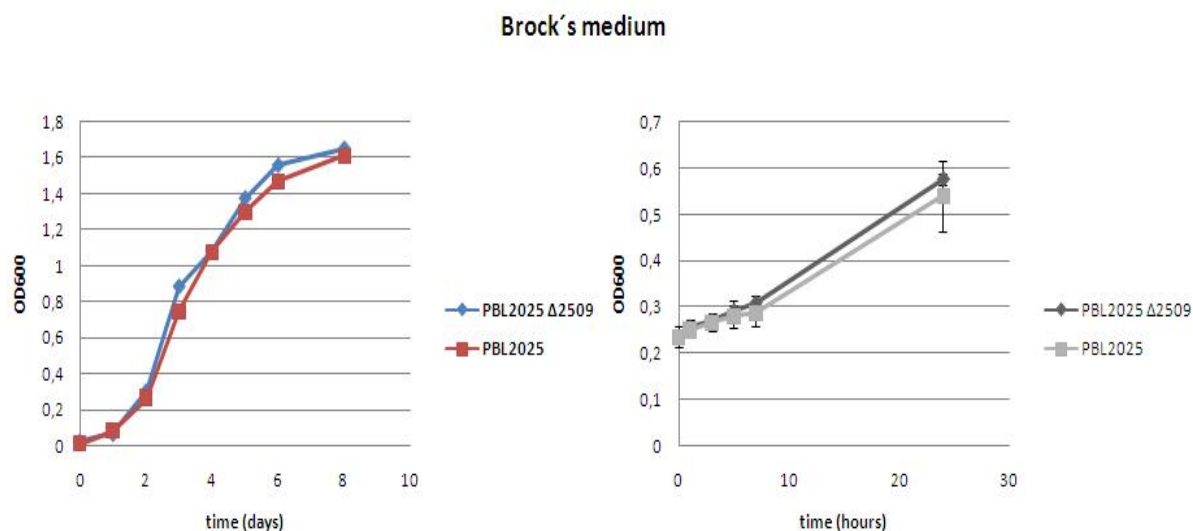


Fig 7. PBL2025 and PBL2025 Δ 2509, were inoculated in Brock's medium (supplemented with 0,2 % N-Z amine and 0,2% sucrose). The cells were incubated at 75°C until they reached stationary phase (9 days, left panel) and then, PBL2025 and PBL2025 Δ 2509 cultures were diluted with fresh medium to an OD₆₀₀ of 0,25 and incubated for 48h. After 0h, 1h, 3h, 5h, 7h and 24h, the OD₆₀₀ was measured (right panel). The values are an average of three independent experiments

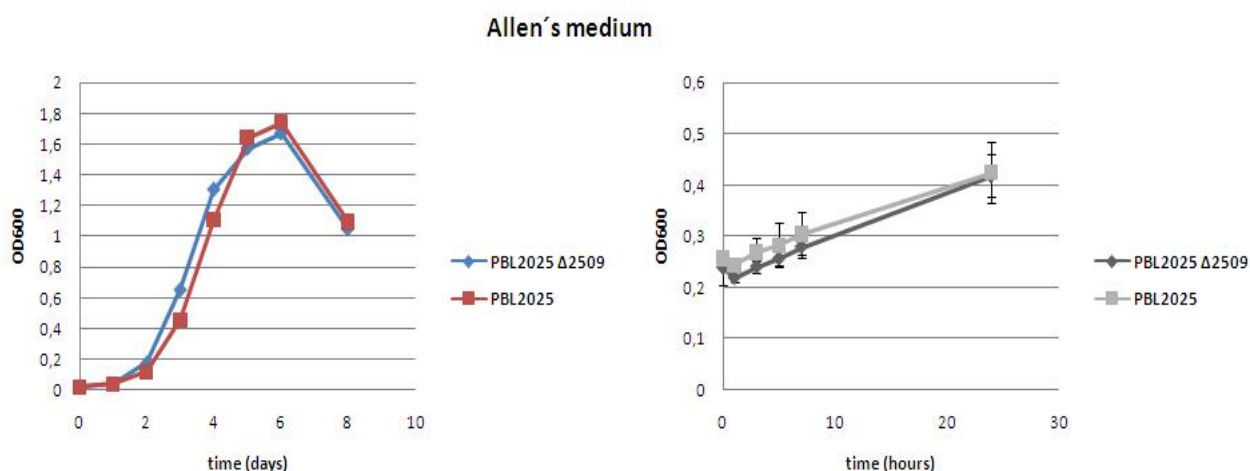


Fig 8. PBL2025 and PBL2025 Δ 2509, were inoculated in 50 ml Allen's minimal medium [10] (supplemented with Wollin's vitamins and 0,2% sucrose). The cells were incubated at 75°C until they reached stationary phase (9 days, left panel). Then, the PBL2025 and PBL2025 Δ 2509 cultures were diluted with fresh medium to an OD₆₀₀ of 0,25 and further incubated for 48h. After 0h, 1h, 3h, 5h, 7h and 24h, the OD₆₀₀ was measured (right panel). The values are an average of three independent experiments

Mediums

Allen's Medium

Allen's Medium [10]	Wollins Vitamines [10]	0,2% sucrose
---------------------	------------------------	--------------

Allens Medium

(NH ₄) ₂ SO ₄ 0.01 M	Fe 4 mg/l
KH ₂ PO ₄ 0.002 M	Mn 0.5 mg/l
MgSO ₄ 0.001 M	B 0.5 mg/l
CaCl ₂ 0.0005 M	Zn 0.05 mg/l
H ₂ SO ₄ ~ 0.001 M	Cu 0.02 mg/l
	Mo 0.01 mg/l
	V 0.01 mg/l

Wollins Vitamines (x100)

d-biotin	2 mg/l
folic acid	2 mg/l
pyridoxine-HCl	10 mg/l
riboflavin	10 mg/l
thiamine-HCl	5 mg/l
nicotinic acid	5 mg/l
DL-Ca-pantothenate	5 mg/l
Vitamine B ₁₂	0,1 mg/l
p-aminobenzoic acid	5 mg/l
lipoic acid	5 mg/l

References

1. Deana, A., H. Celesnik, and J.G. Belasco, (2008) *The bacterial enzyme RppH triggers messenger RNA degradation by 5' pyrophosphate removal*. Nature, **451**(7176): 355-358.
2. Newbury, S.F., (2006) *Control of mRNA stability in eukaryotes*. Biochem Soc Trans, **34**(Pt 1): 30-34.
3. Hasenöhrl, D., et al., (2008) *Translation initiation factor a/eIF2(-gamma) counteracts 5' to 3' mRNA decay in the archaeon Sulfolobus solfataricus*. Proc Natl Acad Sci U S A, **105**(6): 2146-2150.
4. Schelert, J., et al., (2004) *Occurrence and characterization of mercury resistance in the hyperthermophilic archaeon Sulfolobus solfataricus by use of gene disruption*. J Bacteriol, **186**(2): 427-437.
5. Albers, D., (2007) *Conditions for genedisruption by homologous recombination of exogenous DNA into the Sulfolobus solfataricus genome*. Archaea2, 145-149 published online.
6. Albers, S.V., et al., (2006) *Production of recombinant and tagged proteins in the hyperthermophilic archaeon Sulfolobus solfataricus*. Appl Environ Microbiol, **72**(1): 102-111.
7. Jonuscheit, M., et al., (2003) *A reporter gene system for the hyperthermophilic archaeon Sulfolobus solfataricus based on a selectable and integrative shuttle vector*. Mol Microbiol, **48**(5): 1241-1252.
8. Schleper, C., K. Kubo, and W. Zillig, (1992) *The particle SSV1 from the extremely thermophilic archaeon Sulfolobus is a virus: demonstration of infectivity and of transfection with viral DNA*. Proc Natl Acad Sci U S A, **89**(16): 7645-7649.
9. Miller, J.H., (1972) *Experiments in Molecular Genetics*. Cold Spring Harbor Laboratory, Cold Spring Harbor, NY1972.
10. Allen, M.B., (1959) *Studies with Cyanidium caldarium, an anomalously pigmented chlorophyte*. Arch Mikrobiol, **32**(3): 270-277.
11. Brouns, S.J., et al., (2006) *Identification of a novel alpha-galactosidase from the hyperthermophilic archaeon Sulfolobus solfataricus*. J Bacteriol, **188**(7): 2392-2399.

Danksagung

Ich bedanke mich ganz herzlich beim gesamten Laborteam für ein wundervolles Jahr und all jenen, die zur Entstehung dieser Diplomarbeit beigetragen haben. Weiters bedanke ich mich bei Herrn Prof. Dr. Udo Bläsi und Herrn Dr. David Hasenöhrli für die Betreuung meiner Arbeit.

LEBENS LAUF

❖ Persönliche Daten

Name	Lukas Zeichen
Adresse	Rembrandtstrasse 18/12 1020 Wien
Geburtsdatum, -ort	31. Jänner 1984, 9500 Villach
Nationalität	Österreich

❖ Schulausbildung

1991–1995	Volksschule VS 14 9524 St.Magdalen
1995–2003	Bundesrealgymnasium Peral 9500 Villach
2005–2012	Studium der „Molekularen Biologie“ an der Universität Wien

❖ Praktische Erfahrungen

Juli 2001	S-K-M electronics 9800 Spittal (Ferialpraktikum)
2003-2004	Rettungssanitäter Rotes Kreuz Leitstelle 9500 Villach
Februar-März 2005	<i>Sparkassen Versicherung; Camelot</i> Informatik & Consulting GmbH 1010 Wien (Praktikum)
Juli-August 2006	Infineon Technologies 9500 Villach (Ferialpraktikum)
2007-2011	MR Suite Hotel 200m zum Prater bzw. 900m zur Oper; Dr. Rottman GmbH (Rezeptionist)
März-April 2010	Praktikum MFPL Department for Biochemistry, Universität Wien
Wintersemester 2010/11	Tutor für Übungen I A - Mikrobiologie und Genetik (Universität Wien)
Sommersemester 2011	Tutor für Übungen I A - Mikrobiologie und Genetik (Universität Wien)
Wintersemester 2011/12	Tutor für Übung in Molekulare Mikrobiologie (Universität Wien)
Wintersemester 2011/12	Tutor für Übungen I A - Mikrobiologie und Genetik (Universität Wien)
2011-2012	Diplomarbeit (“Characterisation of RNase J in <i>S. acidocaldarius</i> ”) MFPL Department for Mikrobiologie, Immunology and Genetics. Labor Bläsi, Universität Wien